Cell Reports

Article

# Prospective and retrospective representations of saccadic movements in primate prefrontal cortex

## Graphical abstract

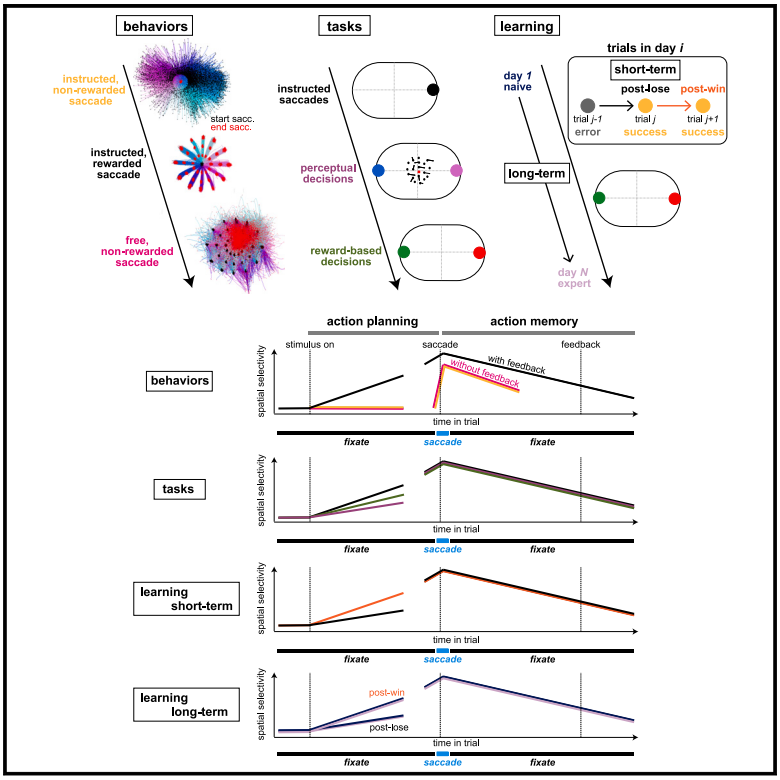


## Highlights

- Retrospective representations maintain the memory of the most recent saccadic movement
- Prospective representations are limited to task-related saccades eligible for rewards
- The link between retrospective and prospective representations is highly structured
- Spatial responses are shaped by trial history but not day-to-day behavioral improvements


## Authors

Ioana Calangiu, Sepp Kollmorgen, John Reppas, Valerio Mante

## Correspondence

calangiu@ini.uzh.ch (I.C.), valerio@ini.uzh.ch (V.M.)



## In brief

Calangiu et al. show that, during oculomotor behaviors, the strongest choice representations in dlPFC encode action memories rather than action plans. These retrospective representations seem to be largely fixed across different behaviors, tasks, and learning time scales, supporting the existence of a predominant, rigid representation of space in the dlPFC.


Calangiu et al., 2025, Cell Reports *44*, 115289
February 25, 2025 
https://doi.org/10.1016/j.celrep.2025.115289

CellPress

Cell Reports

CellPress
OPEN ACCESS

Article

# Prospective and retrospective representations of saccadic movements in primate prefrontal cortex

Ioana Calangiu,[1,*] Sepp Kollmorgen,[1] John Reppas,[2] and Valerio Mante[1,3,*]
[1]Institute of Neuroinformatics and Neuroscience Center Zurich, University of Zurich and ETH Zurich, Zurich, Switzerland
[2]Department of Neurobiology and Howard Hughes Medical Institute, Stanford University, Stanford, CA, USA
[3]Lead contact
*Correspondence: calangiu@ini.uzh.ch (I.C.), valerio@ini.uzh.ch (V.M.)
https://doi.org/10.1016/j.celrep.2025.115289

## SUMMARY

The dorso-lateral prefrontal cortex (dlPFC) contributes to flexible, goal-directed behaviors. However, a coherent picture of dlPFC function is lacking, as its activity is often studied only in relation to a few events within a fully learned behavioral task. Here we obtain a comprehensive description of dlPFC activity across different task epochs, saccade types, tasks, and learning stages. We consistently observe the strongest modulation of neural activity in relation to a retrospective representation of the most recent saccade. Prospective, planning-like activity is limited to task-related, delayed saccades directly eligible for a reward. The link between prospective and retrospective representations is highly structured, potentially reflecting a hard-wired feature of saccade responses. Only prospective representations are modulated by the recent behavioral history, but neither representation is modulated by day-to-day behavioral improvements. The dlPFC thus combines tightly linked flexible and rigid representations with a dominant contribution from retrospective signals maintaining the memory of past actions.

## INTRODUCTION

The dorso-lateral prefrontal cortex (dlPFC) in primates is thought to play a key role in goal-directed behavior by flexibly maintaining and integrating signals required to select contextually relevant actions, through processes like working memory, attention, and the context-dependent accumulation of sensory evidence.[1–7] This view of dlPFC function has been shaped in particular by studies in primates engaged in saccade-based tasks, many of which focused on characterizing responses preceding an action.[8–10] A large literature on pre-saccadic responses revealed neural dynamics that is strongly context dependent,[9,11] can support abstract representations,[7,12–16] and reflects representations of task variables that are randomly mixed at the level of single neurons,[7,17] consistent with a primary role of the dlPFC in the prospective control of flexible decisions.

Prominent task-related activity, however, has often been reported also during[11] and after saccades.[8,11,18–28] One widely reported signal is post-saccadic activity, which in several areas of the dlPFC, is intermingled with pre-saccadic and movement related activity.[8,11,26,27] The proposed functions of post-saccadic activity mostly differ from those of pre-saccadic activity, and include the retrospective monitoring of the behavioral context,[18,24,28,29] terminating cognitive processes that select contextually relevant actions,[30] updating retinotopic maps to ensure visual stability,[23,27,31] or alternatively, the preparation for future actions.[11] Currently, a systematic comparison of the prevalence and properties of pre- and post-saccadic activity across contexts, stages of learning, and neurons is lacking, and consequently the primary function of dlPFC remains a matter of debate.

Here, we compared neural population recordings obtained with chronically implanted electrode arrays in the dlPFC of macaques[32,33] across a variety of behavioral contexts. Such array recordings arguably provide a more unbiased view into the signals represented by a neural population compared with past single-neuron recordings. Monkeys were engaged in several classic, saccade-based motor and decision-making tasks that differed in a critical aspect from past studies.[9,11] Operant saccades were not only preceded, but also followed, by a delay period that was randomized from trial to trial,[28] simplifying a direct comparison between the prevalence and properties of pre-saccadic and post-saccadic representations. To establish the role of behavioral context on the inferred dlPFC representations, we compared neural population responses across tasks, across different stages of learning, and between trained and freely chosen saccades.

We find that the dlPFC can represent saccade direction from the time of planning, through movement, until the resulting outcome and beyond. Notably, the dominant signal across tasks, saccade types, and learning is post-saccadic activity, suggesting a key role of dlPFC in retrospective computations. Our findings are organized in three sections. First, we show that post-saccadic activity overall is stronger than, and distinct from, pre-saccadic activity (Figures 1, 2, and 3). Like pre-saccadic activity, post-saccadic activity is persistent and inherently tuned to the direction of the saccade, but it represents the past rather than the future action.[8,11,18–27] Unlike

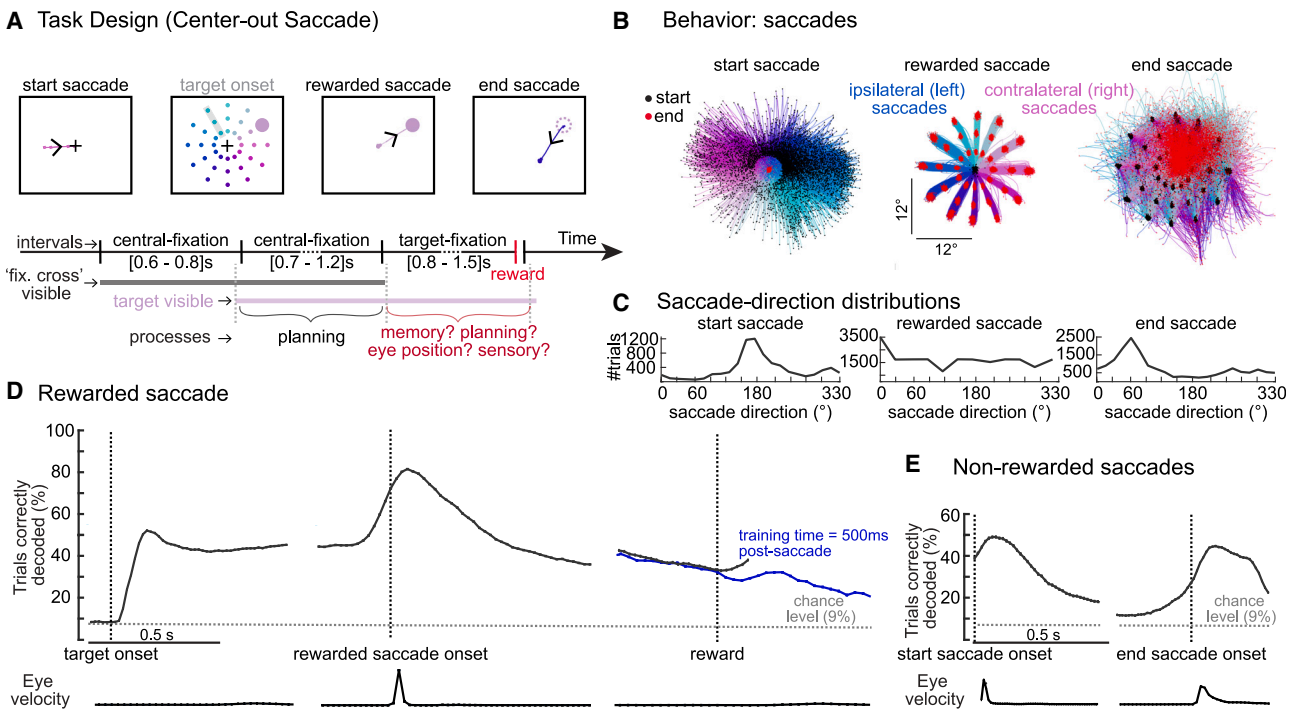


**Figure 1. Instructed saccade task, behavior, and tuned activity**

(A) Task design of the visually guided, delayed saccade task. Here we show 36 unique positions, pooled across all experiments of monkey T, and highlight a direction (3 positions) that was not presented in a particular experiment (in total 33 unique positions per experiment for monkey T and 24 for monkeys V and C, Figure S1C).

(B) Eye trajectories for start, rewarded, and end saccades, sorted by direction. Start and end saccades are discretized to match the rewarded saccade directions from each session.

(C) Saccade direction distribution across all sessions and radii. In approximately 45% of trials, the monkey was at the fixation point at the start, leading to fewer start than end saccades. Only start and end saccades with amplitudes between 4° and 16°, similar to rewarded saccades, are analyzed.

(D) Time-specific decoding of the direction of the rewarded saccade at times aligned to target onset, saccade onset and reward. At each time, a separate multi-class decoder (linear discriminant decoder) is trained and tested on 11 classes (directions). Chance performance is 9%. Eye velocity shows stable fixation prior and post-saccade execution. The blue line indicates decoding accuracy of a single decoder, trained at 500 ms post saccade, and evaluated at many times post reward (only trials where monkeys happen to fixate for longer intervals before the next trial are included).

(E) Cross-validated decoding accuracy when applying the decoders identified for the rewarded saccade (D) to responses aligned to the start (left panel) and end (right panel) saccade.

Decoding accuracies are averaged across all sessions and error bars indicate SEM across sessions ($n$ = 9).

pre-saccadic activity, post-saccadic activity seems to occur in relation to every saccade, albeit with some modulation due to the behavioral context. Second, we show that some components of the identified saccadic representations have tightly linked pre- and post-saccadic dynamics at the single neuron and population level (Figures 4 and 5), consistent with a hard-wired feature of the underlying circuits. Third, we study how the representations of saccade direction are shaped by learning on short[34] (consecutive trials) and long timescales[35] (days and months) in an associative-learning task[21,34] (Figures 6 and 7). Only pre-saccadic representations are influenced by recent trial history, and both pre- and post-saccadic representations show little or no modulation on the longer timescales associated with large changes in behavior. Overall, these findings imply that rigid, structured representations are a key component of dlPFC computations, with a dominant contribution from post-saccadic signals maintaining the memory of past actions.

## RESULTS

### Behavioral task and neural recordings

We first consider recordings from three monkeys that were engaged in a visually guided, instructed saccade task, requiring them to perform a sequence of saccades and fixations on each trial to obtain a reward (Figure 1A). We analyzed neural activity and eye movements for all trial epochs (Figure 1A) and different types of saccades, i.e., the instructed and freely initiated saccades occurring before, during, and after each trial (Figure 1B). We refer to the initial saccade to the fixation point as the "start saccade," the saccade to the target as the "rewarded saccade," and the first saccade away from the target after reward delivery as the "end saccade." Figure 1C shows the distribution of saccade directions for the different saccade types pooled over all experiments and radii (monkey T). The start saccade is followed by the "central-fixation," i.e., the initial fixation on the fixation point lasting for a randomized interval (1.3–2 s) and

preceding the "rewarded saccade." Crucially, the rewarded saccade is followed by the "target fixation," lasting for a randomized interval (0.8–1.5 s), i.e., the fixation on the target until it disappears (Figure S1B). The inclusion of this prolonged target fixation is a key difference from instructed-saccade tasks used in past studies[8,11,26,27,36–39] and greatly simplifies the interpretation of post-saccadic neural activity.

Neural activity was recorded with 96-channel Utah arrays implanted in pre-arcuate cortex, a region of the dlPFC close to, and possibly including, the most rostral part of the frontal eye fields[40] (Figure S1A). Monkeys T and V had the array placed in the concavity of the arcuate sulcus in the left hemisphere, while monkey C had it placed in the right hemisphere, above the principal sulcus.[33] We show results from monkey T and monkey V in the main text. We show results from monkey C in the supplementary figures to highlight similarities and differences from the other monkeys, which may be due to a different array placement. During the duration of an experiment, monkeys were head fixed.

## Tuned post-saccadic activity follows every saccade

We begin our analysis by quantifying the representation of saccade direction in single-trial population responses using cross-validated multi-class decoders[41–46] (Figures 1D and 1E). We decoded the direction of the rewarded saccade from population spike counts at particular times relative to the target onset, the saccade onset and reward delivery.

Cross-validated decoding accuracy varies over time—it increases after the target is presented (Figure 1D, left), peaks after the end of the saccade, persists throughout the target fixation, and is still high at and after reward delivery (up to 2 s after saccade onset). Decoding accuracy late during central fixation and target fixation is comparable (Figure 1D, right; Figures S3B and S3G other monkeys; Figure S2E other decoders). Throughout the central-fixation period, the execution of the rewarded saccade, and the target-fixation period, decoding errors almost exclusively reflect readout directions that are immediately adjacent to the true direction (Figure S2A top row). Decoding accuracy remains high well beyond the time of the saccade, an observation unlikely to be accounted for by transient inputs from motor or sensory areas. Like pre-saccadic activity, post-saccadic activity may thus be a form of persistent, internally generated activity.[8,11,39]

Saccade direction can be robustly read out from the population also after the start and end saccades (Figure 1E, duration of start saccade 54 ms [95% confidence interval (CI), 52–55]; duration of end saccade = 140 ms [95% CI, 125–154]) (Figure S2A, bottom row, and Figure S2B for a finer comparison; Figures S3C and S3H other monkeys). Critically, Figure 1E shows the accuracy of decoders that were trained only on activity around the rewarded saccade, meaning that the same decoders have high accuracy for all three saccades and implying that the population encoding of saccadic activity is largely preserved across different types of saccades. This finding is consistent with representations of saccades in retinotopic coordinates (see also below, Figure 2D).

Neural population activity in pre-arcuate cortex thus seems to encode the direction of a saccade from long before it occurs (for the rewarded saccade) to long after it was completed (for all saccade types). However, the interpretation of post-saccadic activity as a representation of the direction of the immediately preceding saccade is complicated by a feature of the task we analyzed, which is common to many similar tasks. Specifically, the direction of the rewarded saccade is both highly correlated with the direction of the saccade that follows it (the end saccade, which often brings gaze back to the fixation point) (Figure 2A, top right, monkey T; Figures S3A and S3F middle, monkeys V and C) and perfectly correlated with the location of the post-saccadic fixation, i.e., the target location. Unless these correlations are accounted for, it remains unclear whether post-saccadic activity is best explained as representing the direction of the previous saccade, the direction of the next saccade, or the location of the post-saccadic fixation.

Interestingly, recordings in monkey C reveal strong post-saccadic activity but relatively little pre-saccadic activity (Figures S3G and S3H; from a more anterior location in the dlPFC than in monkeys T and V), suggesting that pre- and post-saccadic activity amount to fundamentally distinct signals. Below we reach the same conclusion by analyzing datasets tailored to disambiguate between different possible explanations of post-saccadic representations in monkey T and V, for which both pre- and post-saccadic activity occur in the recordings (Figure 2).

## Post-saccadic activity is not pre-saccadic activity for the next saccade

Two observations indicate that post-saccadic activity is unlikely to represent a plan of the next saccade. First, Figure 1E implies that the end saccade (unlike the rewarded saccade, Figure 1D) is preceded by only very weak predictive activity, which occurs immediately before its execution. This finding suggests that the end saccade is not planned, which in turn implies that any persistent activity following the rewarded saccade is unlikely to represent a saccade plan. Second, we studied whether predictive activity for the end saccade contributes to the strong post-saccadic activity immediately after the rewarded saccade. To this end, we applied a pre-saccadic decoder (defined 150 to 50 ms before the rewarded saccade) to activity after the rewarded saccade, and assessed whether the decoder readout is predictive of the direction of the end saccade.

Notably, we take several steps to ensure that the decoder readout does not simply reflect the correlations between the directions of the rewarded and end saccades. For one, we evaluated the accuracy of the read-outs separately for single directions of the rewarded saccade (rewarded saccades to three contralateral directions are followed by end saccades in many directions and thus suited to test the decoder; Figure 2A, dashed rectangle). For another, we created a balanced test set by sampling an equal number of trials from each end-saccade direction (Figure 2A, bottom right).

With this unbiased approach, we find that throughout much of the target-fixation period a pre-saccadic decoder (blue vertical line, Figure 2B) cannot be used to predict the direction of the

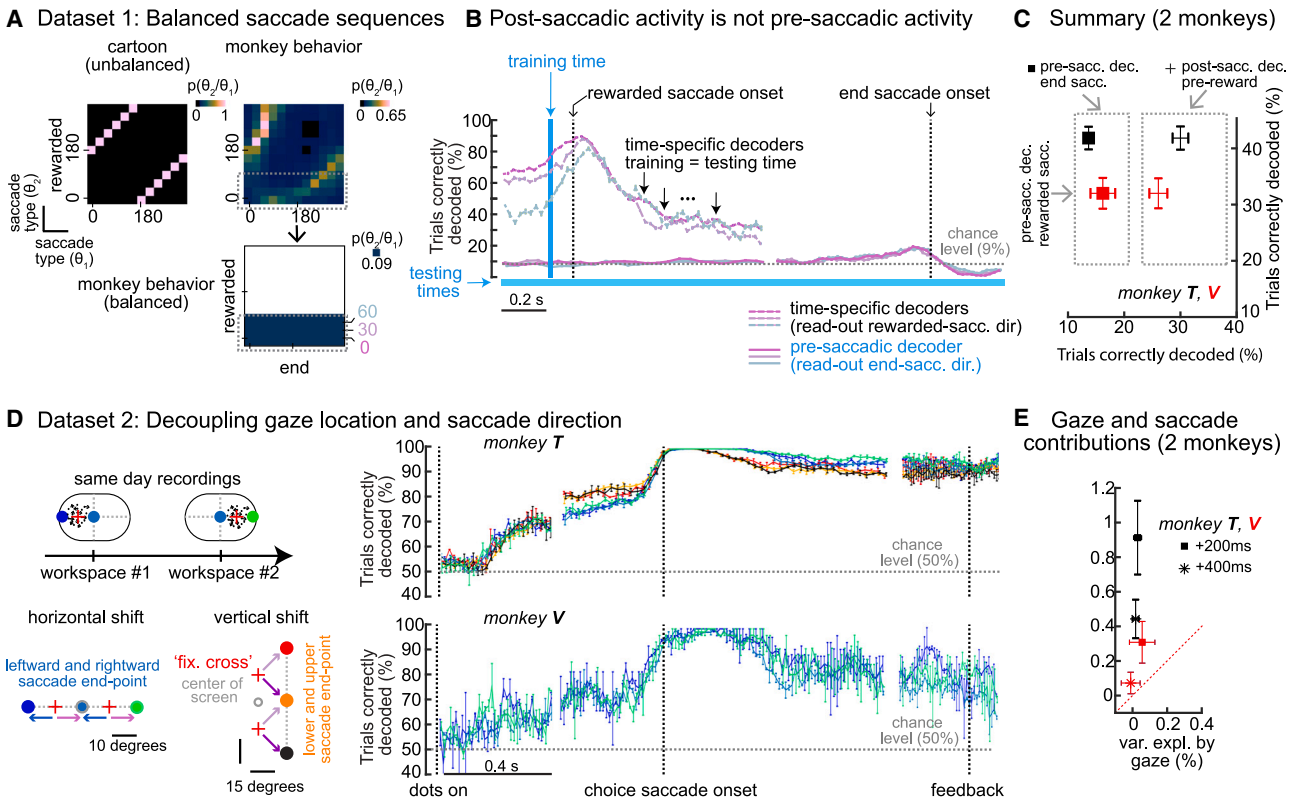


**Figure 2. Nature of representations**

(A–C) Modulations of post-saccadic activity due to future actions. (A) Each panel shows histogram of consecutive saccades, expressed as the distribution of directions for the end saccade (columns) conditioned on the direction of the rewarded saccade (rows). For each row, the sum of columns equals 1. (Left) Synthetic data for an unbalanced set where all end saccades are directed to the fixation point. (Right) Behavior of monkey T. (Bottom) A balanced dataset obtained by resampling trials with rewarded saccades toward 0°, 30°, and 60°.

(B) We apply a decoder trained on responses before rewarded saccade (blue area) to activity after the rewarded saccade separately for the three conditions in the balanced dataset. The resulting readout is not predictive of the direction of the end saccade (bottom three curves). In contrast, on the same set of trials, the direction of the rewarded saccade can be decoded with high accuracy when using the time-specific decoders from Figure 1D (top three curves).

(C) Summary plot. The pre-saccadic activity of the end saccade is much weaker both compared with the post-saccadic activity of the rewarded saccade before reward (compare squares and crosses along the horizontal axis) and to the pre-saccadic activity of the rewarded saccade (squares are above the unit line) ($n = 9$).

(D and E) Non-retinotopic modulations of saccade-related activity. (D) Recordings from a random dots task that included trials from two shifted workspaces, whereby the location of the fixation point in a given workspace was shifted either along the horizontal midline (cold colormap) or along the vertical line (warm colormap). In the vertical shift, both targets were placed in the contralateral hemifield, at 15° and 315°, to elicit high responses. Monkey V has sessions only from the horizontally shifted workspace. (E) Summary plot of saccade and gaze modulation at single-unit level. Saccade direction modulates a larger portion of variance compared with gaze. ($n = 4$, 2 per each shift for monkey T; $n = 2$ for monkey V).

Across all panels, error bars indicate SEM across n sessions.

end saccade (solid lines in Figure 2B, close to chance; colors correspond with the three rewarded saccade directions in the balanced dataset). During the same period, in contrast, time-specific decoders (from Figure 1D) do predict the direction of the preceding rewarded saccade well above chance (dashed lines in Figures 2B and 1D).

We obtained similar results in both monkeys T and V (Figure 2C). Immediately before the onset of the end saccade, predictive activity for the direction of the upcoming end saccade (Figure 2C, horizontal axis, squares) was weak compared with the representation of the direction of the preceding rewarded saccade (Figure 2C, horizontal axis, crosses). Together, the above observations imply that post-saccadic activity, consistently in all monkeys, does not represent the plan of a future action.

## Post-saccadic activity does not encode the momentary gaze location

Two observations indicate that momentary gaze location[43–45,47–52] is also unlikely to be the main contributor to post-saccadic activity. A first indication is given by the finding that post-saccadic decoders trained on the rewarded saccade can also decode the directions of the start and end saccades (Figure 1E, times after saccade onset). Unlike for the rewarded saccade, for these saccades, the correlation between saccade direction and post-saccadic gaze location is reduced or absent. All start saccades, in particular, end on the central fixation point, meaning that the post-saccadic gaze location is identical across all trials. Yet, the direction of the preceding saccade can be decoded with high performance also following start saccades (Figure 1E, left).

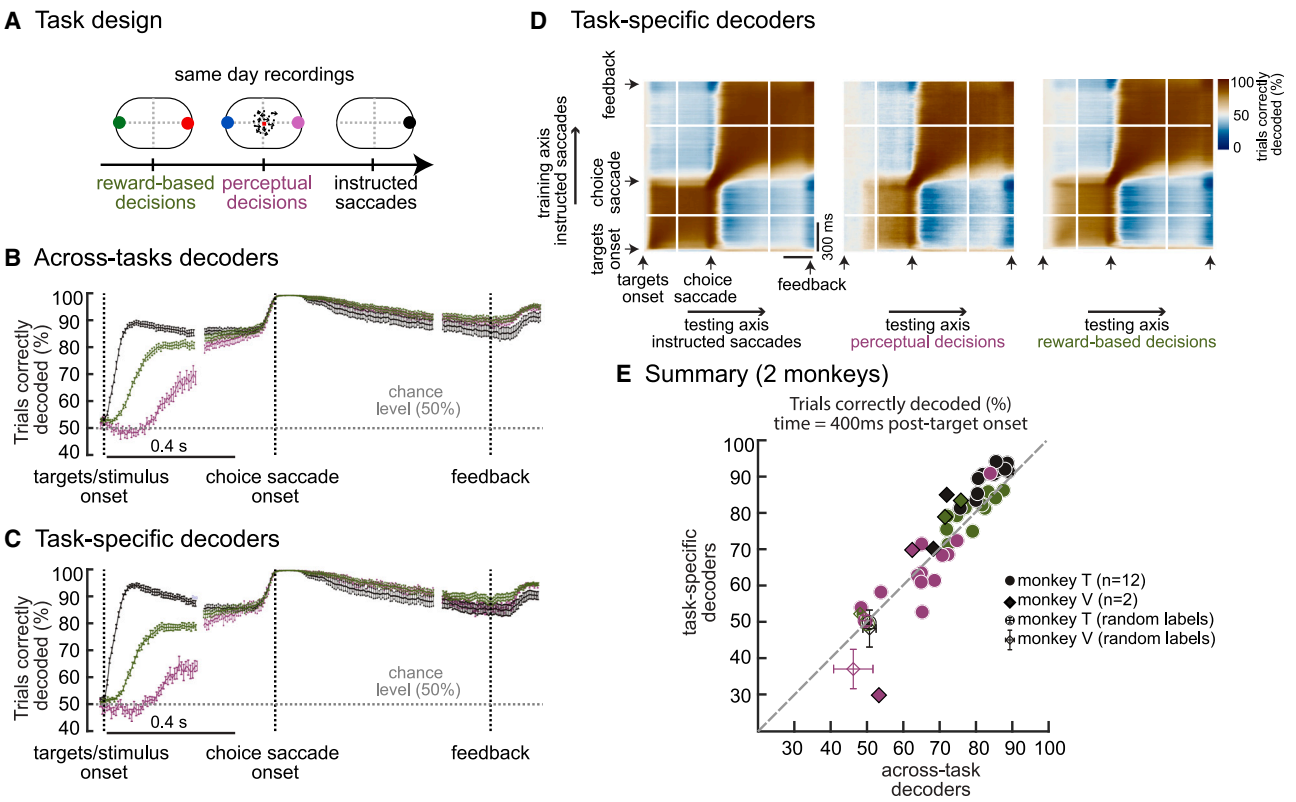


**Figure 3. Different tasks, same patterns of activity**

(A) Same-day recordings with common choice targets for three tasks.

(B) We identify a common support vector machine for choice direction on a balanced set across the three tasks.

(C) We identify decoders for choice direction for each task (task-specific decoders).

(D) We evaluate decoders specific to the instructed saccades from activity from through-out the trial, to perceptual decisions (middle) and reward-based decision (right). Decoding accuracies are averaged across sessions and error bars indicate SEM across sessions ($n$ = 12). Analogous figure for monkey V (Figure S4).

(E) Summary decoding accuracy for both monkeys at 400 ms post target/stimulus onset. Empty markers indicate averaged decoding accuracy when choice labels were shuffled. Decoding accuracies of choice exceed chance levels (50% or empty markers) both for across-task and for task-specific decoders.

We find further evidence that post-saccadic does not primarily represent gaze location in a separate behavioral task, for which we partially decoupled the direction of the rewarded saccade and post-saccadic gaze-location. Each experiment included trials from two shifted workspaces, whereby the location of the fixation point in a given workspace was shifted either to the left or right from the horizontal midline, or above or below the horizontal midline (Figure 2D). As a result, one of the choice targets in this task (Figure 2D, light blue and orange target) was reached with saccades having very different metrics across workspaces.

Even when the post-saccadic gaze location is controlled in this way, the direction of the rewarded saccade can be decoded with high accuracy throughout the central-fixation, movement, and target-fixation periods (Figure 2D, right, for monkeys T and V). In particular, decoding accuracy is high even on trials that all shared the same post-saccadic gaze location (Figure 2D, light blue and orange) and similar to the accuracy on trials where direction and gaze-location covaried (Figure 2D, other colors). This observation alone implies the existence of a strong representation of saccade direction that is independent of any concurrent representation of gaze location. We further quantified the influence of saccade direction and gaze location at the unit level with a linear regression model, whereby each unit's activity is captured as a combination of these two factors. Overall, the previous saccade direction explained a substantially larger fraction of the variance in activity than gaze location[29] (Figure 2E).

The above findings also make it unlikely that post-saccadic activity represents a gaze-dependent visual input. In fact, selectivity to visual inputs is unrelated to post-saccadic selectivity at the unit level (Figure S7C). The most parsimonious interpretation of post-saccadic activity is that it represents a retrospective signal, a short-term memory of the preceding saccade. The strength and time-course of this action memory seems to vary across saccades, as decoding accuracy differs between different types of saccades (Figures 1D, 1E, S3B, S3C, S3G, and S3H). These differences may imply that post-saccadic activity is modulated by contextual influences, like the temporally discounted reward expectation[53] associated with each saccade.

### Prospective and retrospective representations have different task selectivity

We further studied context-dependent modulations by comparing activity preceding and following the rewarded saccade across three tasks that differ in terms of the information guiding saccade planning (Figure 3A for monkey T; Figure S4 for monkey V): instructed saccades, where saccade plans were based on the location of the presented target (as Figure 1, but with only two target locations); perceptual decisions, where saccade plans were based on the direction of the random-dots (as in Figure 2D, but for a single workspace); and reward-based decisions, where saccade plans were based on the choice and outcome of the previous trial.[21,54–56] In the latter task (discussed in greater detail below; see Figures 6 and 7), monkeys had to choose between a red and green target, whereby the rewarded color was fixed within blocks of approximately 10–30 trials, but switched unpredictably between blocks.

We obtained recordings from all three tasks on the same day, whereby the location of the choice targets and of the fixation point was fixed across tasks. We analyzed activity starting from the onset of the visual stimulus that guided the monkeys' choices, i.e., the target onset in instructed saccades and reward-based decisions, and the onset of the random dots in the perceptual decisions (Figures 3B and S4B). To study potential contextual modulations of the underlying representations, we estimated and compared choice decoders that were common across tasks with decoders that were task specific.

Early choice-predictive activity along common decoders was strongly modulated by task-context (Figures 3B and S4B). Predictive activity developed quickly for instructed saccades (black), more slowly for reward-based decisions (green), and slowest for perceptual decisions (purple). We observed these differences even though here we only analyzed trials that were matched for average performance across tasks (e.g., only high-coherency motion trials in the perceptual decisions). In contrast with the strong task dependency at trial onset, choice-related activity around and after saccade onset was not or only weakly modulated by task context.

These differences in decoding accuracy at trial onset are observed also when using task-specific decoders (Figures 3C and S4C). The observed task dependency thus reflects true differences in the strength of the corresponding pre-saccadic representations, as opposed to simply reflecting a sub-optimal decoder that captures patterns of activity that are common across tasks but may not be optimal for some individual tasks. This conclusion is also supported by directly comparing the temporal dynamics of the task-specific decoders[7,17,32,41,57–59] (Figures 3D and S4D). Specifically, we applied the decoders from one task, trained at any given time in the trial, to activity recorded at all times either in the same task (Figure 3D left) or in a different task (Figure 3D, middle and right). This analysis revealed that early choice-related activity is largely explained by a single, stable component that is similar across tasks, but emerges later in the perceptual and reward-based decisions (Figure 3D middle and right vs. left; Figure S4D). Later, peri- and post-saccadic activity instead undergoes essentially identical dynamics in all tasks (Figure 3D). Consistently in both monkeys (Figure 3E), choice representations thus transition between the same patterns of activity in all tasks, albeit with somewhat different speeds (Figure 3B).

### Prospective and retrospective signals are mixed in individual units

Having established that dlPFC populations maintain prospective and retrospective representations of saccade direction, we asked how these representations are organized at the unit level. In particular, prospective and retrospective signals could be maintained by separate populations of neurons or could be mixed within a single population. To address this question, we focus on the instructed saccade task shown in Figure 1. An examination of example units shows substantial variability across the population in the temporal dynamics of saccade-modulated activity[8,11,27,36–39,60] (Figure 4A), with some units selective before saccade (units #2 and #5), after the saccade (units #7 and #9), or both before and after the saccade (units #1 and #4).

To quantify the strength and dynamics of directional selectivity in individual units, at any given time in the trial we fitted a bell-shaped function to the activity averaged by target direction,[11] while ignoring target eccentricity (Figure 4B). We considered a unit to be direction selective at a particular time if the cross-validated r-squared value of the corresponding fit was higher than 0, i.e., the model describes the direction-averaged responses better than a constant. For selective units, we then defined the preferred direction as the corresponding model parameter (the peak location of the fitted tuning curve).

We find that a substantial fraction of units encodes direction at any given time in the trial in all monkeys (Figure 4C, top for monkeys T and V; Figure S7B for monkey C). The fraction of selective units varies throughout the trial, largely mimicking the time-course of the population-level decoders (Figures 1D; Figures S3B and S3G for monkeys V and C). To compare the strength of tuning in individual units across time, we defined a cross-temporal selectivity measure (Figure 4C, bottom row), which quantifies the percentage of units that are direction selective at a given reference time (small circles on top and curve of the corresponding color), as well as at a different comparison time (horizontal axis).

The cross-temporal selectivity is broadly consistent with mixed selectivity.[59,61,62] A substantial fraction of units that are selective after the saccade are also selective before the saccade or right after target onset (approximately 50% and 25% in monkeys T and V) (Figure 4C, green curves; circles indicate significant cross-temporal selectivity). Similarly, many units that are selective after the target onset or before the rewarded saccade are selective also long after the saccade (Figure 4C, purple curves). Such units are mixed selective, as their activity encodes at least two different signals, namely a prospective action plan and a retrospective action memory. We next tested whether these signals are mixed randomly in single neurons or in a structured way.[61]

### Signal mixing within units is not random

The relationship between prospective and retrospective representations in individual units is highly structured. In units showing both pre- and post-saccadic tuning (Figure S7A), we computed the angular difference between the preferred direction estimated immediately before saccade onset (−100 ms) and two times

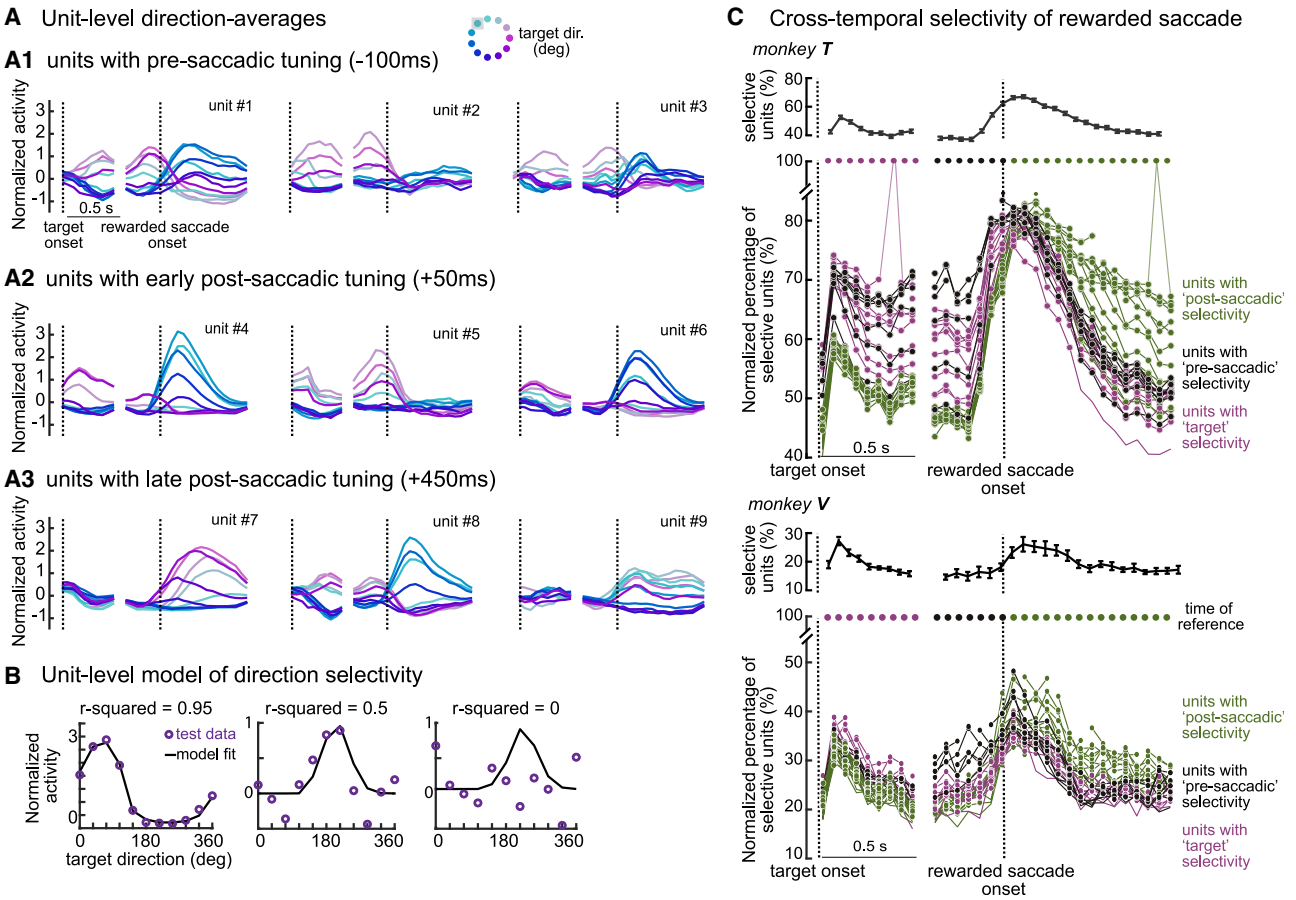


**Figure 4. Saccade-related activity in prefrontal units**

(A) Example direction-averaged responses for units with high goodness-of-fit (r-squared) before (A1), immediately after (A2), and long after the saccade (A3) (target eccentricity is ignored). Black dashed line indicates event onset. Gray area in legend of the target dir. indicates the direction that was not present for this experiment.

(B) Three example fits of the model of direction selectivity to condition-averaged responses with different selectivity levels: from left (highly selective, high r-squared) to right (not selective, r-squared = 0) using cross-validation.

(C) Time-dependent selectivity for the rewarded saccade, showing the percentage of selective units (r-squared > 0) aligned to target (left) and saccade onset (right). (Bottom row) Cross-temporal selectivity, showing the percentage of units selective at a reference time (colored circles) and other times (x axis), normalized to the percentage of selective units at the reference time. For each curve, the lines connecting the corresponding reference time and the two immediately adjacent times (dashed) are mostly omitted.

Circles mark significant cross-temporal selectivity (exceeding 95th percentile of null distribution from 1,000 permutations).

Error bars on top row indicate SEM across sessions.

following the end of the saccade (+50 ms and +150 ms after saccade onset). In monkeys T and V, more units than expected by chance show an angular difference close to 180°, implying that the preferred direction tends to flip between pre- and post-saccadic activity (Figure 5A).

The flip in preferred direction is also prominently reflected in the inferred population decoders. Applying a pre-saccadic decoder trained during the central-fixation to the activity in the post-saccadic epoch results in a pattern of readout errors strongly biased toward the direction opposite to the true saccade direction (Figure 5B, upper row, pre-saccadic decoder; decoding error = 180°). The bias is strongest shortly after completion of the rewarded saccade, but persists throughout even the longest target fixations (Figure S2C).

Similar readout errors are observed when applying the same pre-saccadic decoder to the post-saccadic activity of both the start saccade and end saccade (Figure 5B, middle and bottom rows). Crucially, the prominent regularities in the metrics of saccades that follow the rewarded saccade (Figure S6 for monkey T; end saccades tend to be opposite to the rewarded saccade; Figure S3A for monkey V) are largely absent for the start and end saccades (Figure S6, left and right), implying that the inferred structure between pre and post-saccadic selectivity is not simply a consequence of these regularities in the behavior.

Overall, the relation of pre-saccadic and post-saccadic responses is far from random (Figure 5C, summary for monkeys T and V), but rather reveals a highly structured way for the neural

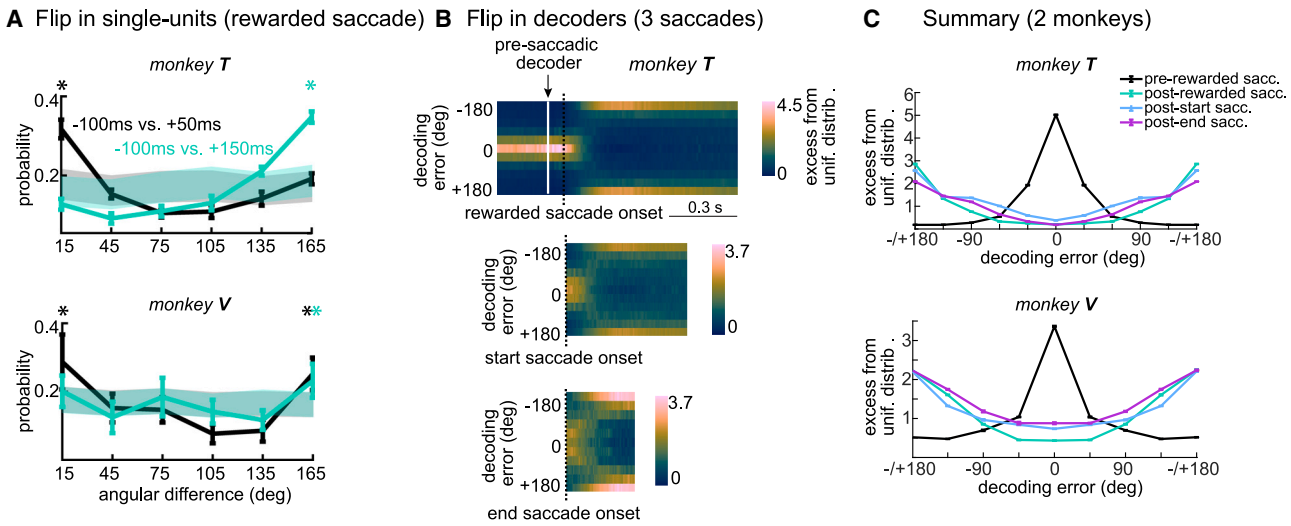


**Figure 5. The relation between pre- and post-saccadic activity**

(A) Histogram of angular difference between the pre-saccadic and post-saccadic preferred directions units that are selective at both times. We shuffle unit orders to create a null distribution, assuming no relation in preferred direction. Shaded areas indicate the 5th and 95th percentiles from 1,000 repetitions. Angular differences are binned in 30°. At +50 ms, pre- and post-saccadic directions match (peak, 15°, stable) and by +150 ms, directions flip (peak, 165°).

(B) Time-dependent histograms of decoding errors of a pre-saccadic decoder (trained on responses from −150 ms to −50 ms before rewarded saccade, Linear Discriminant decoder) when applied onto post-saccadic responses of the rewarded saccade (top), start saccade (middle), and end saccade (bottom). Histograms are normalized with uniform distributions estimated from 1,000 angular differences computed from random discrete values matching target locations. The y axis shows empirical values divided by the uniform mean. Dashed black line indicates saccade onset.

(C) Summary plot showing decoding errors of a pre-saccadic decoder applied to pre-saccadic (−150 ms to −50 ms) and post-saccadic (250–350 ms) responses. Errors are shown only for contralateral saccades because of their strong pre-saccadic activity (Figure S2D for monkey T; Figure S3B for monkey V). The best performing decoder per monkey is used, with results consistent across decoders.

All figures contain results averaged over sessions. Error bars indicate SEM across sessions.

population to transition from representing the plan of an action to representing its memory. These structured representations stand in contrast to the findings of prior studies showing that many abstract variables are randomly mixed across units,[7,17] implying potentially different encoding strategies for spatial and abstract variables.

## Effects of learning on choice representations

Activity in PFC has often been found to be shaped by learning on multiple timescales, from activity modulation reflecting behavioral adjustments between subsequent trials, to the gradual emergence of new representations over many trials of exposure to a new task. Such learning-related effects establish a correlation between neural activity and behavior and can help in constraining the possible functions of the underlying neural representations.

We studied how the identified prospective and retrospective saccade representations change throughout learning in the associative learning task[21] briefly introduced above (Figure 3). Accurate performance in this task was previously shown to rely on an intact pre-arcuate gyrus.[63] Monkeys were engaged in a two-alternative, forced-choice task that required them to track which of two targets (red or green) was being rewarded at any given time (Figure 6A). Because the timing of switches in rewarded color was unpredictable, the optimal strategy is "win-stay, lose-switch"[54–56]: if a given color was rewarded (win), the monkey should choose the same color again on the next trial (stay). Instead, after a choice that was not rewarded (lose), the monkey should switch to the other color (switch). The location of the red and green targets was chosen randomly on each trial. Monkeys' performance gradually improved over the course of many weeks of exposure to this task (Figure 6B).

Achieving optimal performance in this task requires both fast and slow learning.[64] On the fast timescale of trials, monkeys must update their beliefs about what color and location will be rewarded on the current trial based on the actions and outcomes on the preceding trials. On the slow times scales of days and weeks, monkeys must infer the task rules and learn a strategy to optimally harvest rewards. We characterized fast learning with logistic regression models fit to the behavior in a single session, and then studied how the behavioral strategies inferred by the single-session models are shaped by slow learning across sessions (Figure 6C).

For each session, we fitted two separate regression models to explain choice on a given trial based on choice and outcome on the previous trial. The first model only considered the task-relevant target color and predicted the probability to stay on the previously chosen color after a rewarded win trial and the probability to switch color after an unrewarded lose trial (Figure 6C, circles; horizontal and vertical axes: win-stay and lose-switch probabilities). The second model only considered the task-irrelevant target location and similarly predicted the probability to stay or switch location after a win or lose trial (Figure 6C, squares).

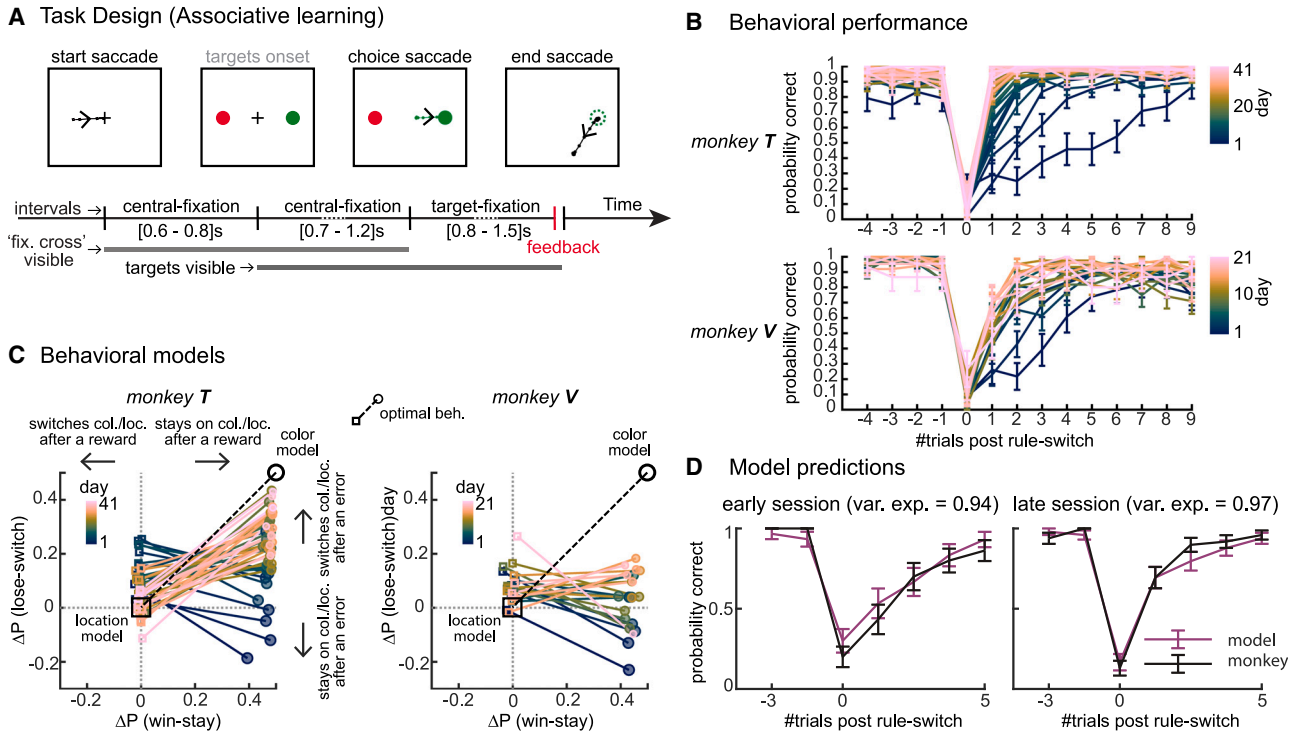


**Figure 6. An associative task and behavior performance**

(A) Task design of the associative task with similar trial structure as the instructed saccade task in Figure 1A. Reward contingencies depend on the previous trial's outcome and chosen color, with color location mapping randomized each trial.

(B) Behavior varies significantly after rule-switch trials, indicating changes in post-error behavior during learning, while post-reward behavior remains consistent.

(C) Estimated probabilities that the monkeys will either choose the same choice-color/choice-location as in the previous trial following rewarded trials (win-stay, horizontal axis) or switch following error trials (lose-switch, vertical axis). Probabilities are corrected by simulated probabilities of a random strategy, where for an optimal agent (black cartoon) ΔP for location is 0 and for color is 0.5.

(D) Simulated color choices using the model of previous relevant history explain well behavior around rule switches, both early and late in training.

Error bars indicate SEM across trials.

From these estimated probabilities, we subtracted the probabilities obtained from simulations of a random strategy. The resulting relative probabilities (ΔP) (Figure 6C) are robust to deviations from complete randomness in the statistics of rule switches, which are inevitable due to the limited number of trials in a session. If monkeys were using an optimal strategy, their choices would be fully determined by color alone (Figure 6C, black circle; corresponding with p[win-stay] = 1 and p[lose-switch] = 1), whereas location would have no predictive power (Figure 6C, black square, corresponding with p[win-stay] = 0.5 and p[lose-switch] = 0.5).

In both monkeys, slow learning primarily involved changes in how monkeys reacted to lose trials, but almost no change in how they reacted to win trials (Figure 6C, over sessions, both circles and squares move substantially along the y axis, but almost not along the x axis). As required by the optimal strategy, monkeys learned to consistently switch colors after a loss trial (Figure 6C, circles; ΔP[lose-switch] increases over days, approaching the optimal value of 0.5). Notably, both monkeys behaved close to optimally after win trials throughout learning, in that they consistently stayed on the rewarded color (Figure 6C, circles; ΔP[win-stay] close to 0.5) and were unaffected by the rewarded location (Figure 6C, squares; ΔP[win-stay] close to 0) already in the first few sessions of this task (Figure 6C, blue colors). In monkey T, learning also involved overcoming an incorrect spatial strategy—monkey T initially tended to switch location after lose trials (Figure 6C left, squares; ΔP[lose-switch] > 0 during early sessions, blue colors) but then progressively learned to ignore the unrewarded location in the subsequent choice (Figure 6C left, squares; ΔP[lose-switch] close to 0 during late sessions, pink colors).

For both monkey, the inferred stay and switch probabilities were sufficient to explain the dynamics of performance after a change in the rewarded color (Figure 6D, measured learning curves vs. simulations based on the regression models), implying that fast learning primarily relies on information from the immediately preceding trial. To characterize the effects of learning on neural activity, we thus compared decoding accuracy for the direction of the choice saccade (choice location) across trials differing in the outcome of the immediately preceding trials (Figure 7A; fast learning) and across early and late sessions (Figure 7B; slow learning). Despite its task relevance, choice color was only weakly represented in the recorded areas (Figure S9).

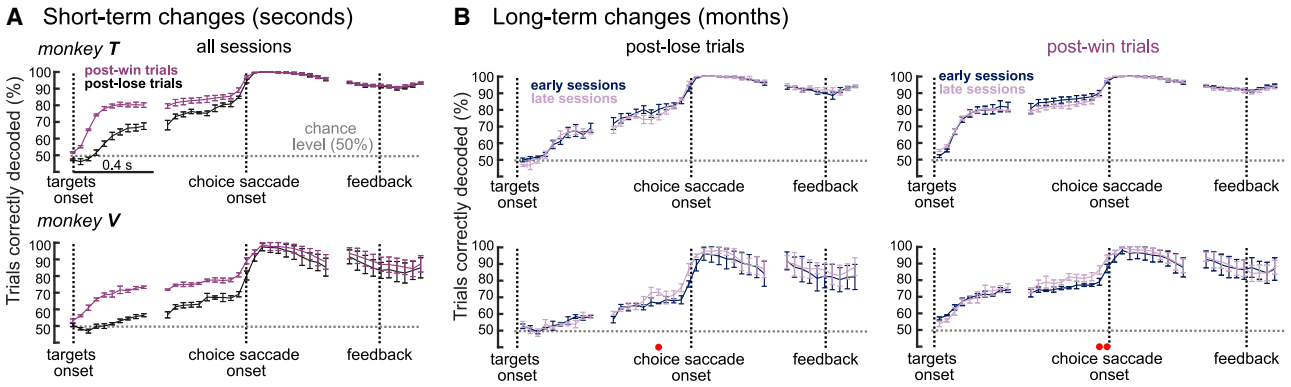


**Figure 7. Choice representations during learning**

(A) Decoders are trained only on post-win trials, i.e., trials after rewarded trials, and evaluated on (1) post-lose trials, i.e., trials after unrewarded trials, and (2) on a held-out set of post-win trials. We resample trials to have the same train and test set size across training days. Decoding accuracy is averaged over all sessions and error bars indicate SEM ($n$ = 36 for monkey T and $n$ = 21 for monkey V).

(B) Decoding accuracy of post-lose trials split for early (first half) and late (second half) training days. Dots indicate a $p$ value of <0.05 (corrected for multiple comparisons) as estimated from a partial correlation that correlates training half (1 for early and 2 for late) and decoding accuracy of each session, controlling for radius (continuous values) and target configuration (one-hot encoding).

(C) Same as (B), but for post-win trials.

Saccadic representations in the dlPFC revealed a potential neural correlate of fast learning, but were strikingly stable over the longer timescales involved in slow learning. Pre-saccadic activity was strongly modulated by the outcome of the immediately preceding trial—choice predictive activity was substantially weaker on trials that followed a loss trial (post lose) compared with those following a win trial (post win; Figure 7A, black vs. purple). This difference between post-win and post-lose trials at the level of neural representations may be a correlate of the different behavioral strategies applied on these trials—consistently across sessions, monkeys tended to stay on the same color on post-win trials (Figure 6C, circles close to 0.5 along the x axis) and tended to switch color on post-lose trials (Figure 6C, circles above 0 along the y axis). However, the same neural representations failed to reveal any correlates of slow learning. Whereas behavioral strategies after lose trials change throughout learning (Figure 6C, positions of circles and square vary along y axis), neither post-win nor post-lose saccadic representations were modulated between early and late sessions (Figure 7B, black vs. purple). The representation of other task variables, like choice color, was also mostly unchanged throughout learning (Figure S9B). Overall, the properties of pre- and post-saccadic representations thus seemed to be largely fixed over long timescales, and only pre-saccadic representations seemed to be correlated with fast learning.

## DISCUSSION

We measured and quantified population activity in pre-arcuate cortex of macaque monkeys across different tasks (instructed, perceptual discrimination, and reward-based decisions), different type of saccades (instructed and free), and different learning timescales (seconds and months) to obtain a comprehensive characterization of saccade-related activity in the pre-arcuate cortex in different contexts.

### Properties of pre- and post-saccadic activity

We find that post-saccadic activity is the strongest and most consistent form of saccade-related activity, both at the unit level (Figure 4C, top row for monkeys T and V; Figure S7B for monkey C) and at population-level (Figures 1D and 1E for monkey T; Figures S3B and S3G for monkeys V and C). The direction of the rewarded saccade can be best decoded after the saccade is already completed, and decoding performance remains high until the time of feedback, throughout a delay period during which the gaze is fixed (Figure 1D). This finding is notable in an area of the dlPFC that was previously primarily associated with pre-saccadic responses.[65] A key factor in revealing the prominence of post-saccadic activity was to more closely balance the duration of pre- and post-saccadic epochs in our tasks.

The persistence of post-saccadic activity seems at odds with the findings of some previous studies, which instead reported largely transient activity.[8,30] These past studies, however, did not include a temporal separation between the saccade and the feedback. The persistent nature of post-saccadic activity might become apparent only when such a delay period is included in the task, since any task-relevant saccade-related information may have to be maintained until feedback is provided.

As in more posterior areas of the PFC,[8,11,26,27] but not more anterior ones,[24,25] post-saccadic activity is intermingled with pre-saccadic and movement-related activity (see Methods S1 for more discussion on retinotopic coordinates). When pre- and post-saccadic activity co-occurs in single neurons, they are tightly linked—the preferred direction typically flips by 180° between the pre- and post-saccadic epochs for all saccades (Figure 5). Analogous flips in selectivity have been observed before in relation to saccades,[8,11] but may also occur in other settings.[32,66,67] This structure stands in contrast with the common finding that in associative areas task-related variables are often randomly mixed in the population.[7,17,59] As discussed

below, one possible function of the observed flips may be to update a representation of visual space across saccades.

Pre- and post-saccadic activities are differently modulated by saccade type and task. Unlike pre-saccadic activity[11,26,38,68] (but see Sendhilnathan et al.[69]), post-saccadic activity occurs after every saccade, but is strongest and lasts the longest after rewarded saccades (i.e., the last saccades preceding feedback and reward delivery) (Figure 1D). Weaker and more short-lived post-saccadic activity follows the start saccades that initiate a trial, and the end-saccades that follow the reward (Figure 1E).

During learning, we find that choice representations reflect the recent trial-to-trial history, but not day-by-day behavioral improvements. The lack of change on the timescale of days was particularly surprising for trials following errors, where the behavior strongly changes throughout the learning process. The fast adjustment to rule switches in later sessions (pink lines in Figure 6B) indicate that monkeys correctly interpret errors as informative factors relevant for future decisions. Nevertheless, the weak choice representations on post-error trials are observed in late and early sessions, despite an almost impeccable behavioral performance during late sessions. Such weaker predictive activity[70] may reflect a number of processes, including lower confidence, more frequent changes of mind,[71] or a slower decision dynamics after negative feedback.[72,73] The task structure, as well as the reward schedule, i.e., how reliable is the stimulus-response-outcome association, can however affect how outcome history affects the encoding of previous and future choices.[74] Together, these results reveal that the dlPFC is susceptible to such contextual associations imposed by external factors (the current choice depends on the previous choice or not; the stimulus-choice-outcome association is fixed or volatile), but not to behavioral adjustments aimed at exploiting these associations (errors due to own mistakes vs. errors due to changes in the statistics of the external world).

The fact that a linear decoder was capable of reading the monkey's choice independent of the task (Figure 3B) suggests that the dlPFC constitutes an advanced processing stage where representations are rather rigid and resemble domain-general[75] and/or untangled[76] representations. These representations did not reflect the large changes in behavior occurring while monkeys learned the reward-based decisions. This task learning[77] could instead reflect plasticity in areas upstream of the dlPFC or in recurrent circuits involving both cortical and subcortical areas.[78]

## Possible functions of post-saccadic activity

The finding that post-saccadic activity amounts to an action memory is consistent with a key role of the dlPFC in retrospective monitoring of behavioral context and in binding the past to the present[18,19,21,24,25,28,29,79,80] (see Methods S1 for a detailed overview of previously proposed functions). The persistent representation of an action memory may be similar to the maintenance of other behaviorally relevant variables in working memory (e.g., Miller et al.,[3] Mante et al.,[7] and Tsujimoto et al.[81]). Representations of past stimuli in dlPFC, however, are not limited to persistent activity, but can remain present in activity-silent traces that reappear as activity on future trials.[82] Temporary records of previous actions are required by many reinforcement learning algorithms to evaluate the actions' relevance with respect to rewards[25,78,83–86] (see the supplemental discussion on choice memories[87–90] and eligibility traces). Neither pre- nor post-saccadic activity was modulated by slow learning processes, suggesting that the underlying spatial representations are a rigid, core feature of the dlPFC. Such rigid representations may coexist with the flexible emergence of representations of abstract task variables.[7,12,59,91,92] The separation of rigid and flexible representations could be computationally advantageous, as it might reduce task interference[93] or catastrophic forgetting.[93,94]

Beyond learning, post-saccadic activity could contribute to updating representations of visual space in PFC and to maintaining visual stability across saccades.[27,95,96] Our own work and previous studies implies that visual stimuli, salient locations, action plans, and their memories are all represented in the dlPFC in maps organized in retinotopic coordinates.[11,27,38] Any behavior requiring more than a single saccade, like the visual exploration of a scene, or the execution of sequences of saccades to multiple remembered locations, requires updating these retinotopic maps following each saccade, a process often referred to as remapping.[23,97–101] Concretely, after a saccade, a retinotopic map needs to be updated by shifting it along a vector that is the exact opposite of the vector of the saccade that was just executed (Figures S10 and S13 in Goldberg et al.[27]). The prominent flip in direction selectivity observed after each saccade could quickly[31] provide such an update signal or could reflect the outcome of the update process.

A contribution of post-saccadic activity to updating spatial representations would imply a critical role for PFC in predicting and compensating for the consequences of one's own actions.[95,96,102,103] Consistent with such a role, impairments in generating and incorporating predictions are thought to be a defining feature of schizophrenia,[104,105] which consistently involves prominent changes in prefrontal circuits[105,106] as well as an impaired ability to generate long and frequent saccades in visual exploration.[107]

## Conclusion

Pre-arcuate cortex actively maintains accurate, persistent representations of saccades before, during, and after each saccadic movement. The representations of saccadic action plans and saccadic action memories are expressed in the same frame of reference, retinotopic coordinates, making them well suited as a basis for reinforcement learning algorithms[108] and for the computations underlying visual stability across saccades.[95] The observed, concurrent representations of saccadic action preparation, action execution, and action memories support a prominent role of PFC in linking events across time. An important question for future studies is how the strong and rigid spatial representations we described relate to the flexible representations of more abstract behavioral variables in PFC and throughout the brain.[24,25,109,110]

## Limitations of the study

Our current study focuses on analyzing many types of saccades during the trial. Additional studies where action and outcome are separated not just by time, but also by intervening actions, will help to elucidate how action memories and action plans are

integrated toward future goals. Furthermore, we study prefrontal responses during learning in a task where one key component of learning involves overcoming an initial (incorrect) spatial strategy. Longitudinal recordings in tasks involving both abstract and spatial learning are needed to further test how long-term learning influences the different types of representations in prefrontal cortex.

## RESOURCE AVAILABILITY

### Lead contact

Requests for further information and resources should be directed to the lead contact Valerio Mante at (valerio@ini.uzh.ch).

### Materials availability

This study did not generate new unique reagents.

### Data and code availability

- All neural data used in this paper are available at https://doi.org/10.5281/zenodo.14360532.
- Custom software used in the above analyses will be made available upon reasonable request to the lead contact.
- Any additional information required to reanalyze the data reported in this paper is available from the lead contact upon request.

## ACKNOWLEDGMENTS

We thank W. T. Newsome for providing us the data and for discussions on the results. We also thank members of the Mante Lab for valuable feedback throughout the project. This work was supported by the Swiss National Science Foundation (SNSF Professorship PP00P3-157539 to V.M.), the Simons Foundation (award 328189 to W. T. Newsome and V.M., and 543013 to V.M.), the Swiss Primate Competence Center in Research, the Howard Hughes Medical Institute (through W. T. Newsome), the DOD | USAF | AFMC | Air Force Research Laboratory: W. T. Newsome, agreement number FA9550-07-1-0537 (V.M. and J.R.), the University Research Priority Program (URPP) 'Adaptive Brain Circuits in Developing and Learning (AdaBD)' (V.M.), and University of Zürich Forschungskredit Grant 'Candoc' (I.C.).

## AUTHOR CONTRIBUTIONS

I.C. and V.M. designed the study and the methods. J.R. conceived and conducted the experiments and collected the data. I.C. performed the analyses, with input from V.M. and assistance from S.K. S.K. provided software for data visualization and data pre-processing. I.C., V.M., and S.K. wrote the manuscript. All authors were involved in discussing the results and the manuscript.

## DECLARATION OF INTERESTS

The authors declare no conflict of interests.

## STAR★METHODS

Detailed methods are provided in the online version of this paper and include the following:

- KEY RESOURCES TABLE
- EXPERIMENTAL MODEL AND SUBJECT DETAILS
- METHOD DETAILS
  - Behavioral tasks
  - Neurophysiological recording
- QUANTIFICATION AND STATISTICAL ANALYSES
  - Analysis of eye movement data
  - Analysis of behavioral data in the non-spatial associative task
  - Task epochs used for analysis of neural data
  - Analysis of single-unit responses
  - Decoding analysis of population responses
  - Post-saccadic activity is not pre-saccadic activity for the next saccade
  - Prospective and retrospective representations have different task-selectivity
  - Post-saccadic activity does not encode the momentary gaze location

## SUPPLEMENTAL INFORMATION

Supplemental information can be found online at https://doi.org/10.1016/j.celrep.2025.115289.

Received: August 26, 2022
Revised: November 24, 2024
Accepted: January 17, 2025
Published: February 12, 2025

## REFERENCES

1. Mansouri, F.A., Tanaka, K., and Buckley, M.J. (2009). Conflict-induced behavioural adjustment: a clue to the executive functions of the prefrontal cortex - PubMed. Nat. Rev. Neurosci. *10*, 141–152.
2. Fuster, J.M. (2008). The Prefrontal Cortex (Academic Press/Elsevier).
3. Miller, E.K., and Cohen, J.D. (2001). An Integrative Theory of Prefrontal Cortex Function. Annu. Rev. Neurosci. *24*, 167–202. https://doi.org/10.1146/annurev.neuro.24.1.167.
4. Duncan, J., and Miller, E.K. (2002). Cognitive Focus through Adaptive Neural Coding in the Primate Prefrontal Cortex. In Principles of Frontal Lobe Function (Oxford University Press), pp. 278–291. https://doi.org/10.1093/acprof:oso/9780195134971.003.0018.
5. Fuster, J.M. (2001). The prefrontal cortex–an update: time is of the essence. Neuron *30*, 319–333. https://doi.org/10.1016/S0896-6273(01)00285-9.
6. Duncan, J. (2001). An adaptive coding model of neural function in prefrontal cortex | Nature Reviews Neuroscience. Nat. Rev. Neurosci. *2*, 820–829.
7. Mante, V., Sussillo, D., Shenoy, K.V., and Newsome, W.T. (2013). Context-dependent computation by recurrent dynamics in prefrontal cortex. Nature *503*, 78–84. https://doi.org/10.1038/nature12742.
8. Funahashi, S., Bruce, C.J., and Goldman-Rakic, P.S. (1991). Neuronal activity related to saccadic eye movements in the monkey's dorsolateral prefrontal cortex. J. Neurophysiol. *65*, 1464–1483. https://doi.org/10.1152/jn.1991.65.6.1464.
9. Funahashi, S., Bruce, C.J., and Goldman-Rakic, P.S. (1989). Mnemonic coding of visual space in the monkey's dorsolateral prefrontal cortex. J. Neurophysiol. *61*, 331–349. https://doi.org/10.1152/jn.1989.61.2.331.
10. Fuster, J.M., and Alexander, G.E. (1971). Neuron activity related to short-term memory. Science *173*, 652–654. https://doi.org/10.1126/science.173.3997.652.
11. Bruce, C.J., and Goldberg, M.E. (1985). Primate frontal eye fields. I. Single neurons discharging before saccades. J. Neurophysiol. *53*, 603–635. https://doi.org/10.1152/jn.1985.53.3.603.
12. Asaad, W.F., Rainer, G., and Miller, E.K. (1998). Neural Activity in the Primate Prefrontal Cortex during Associative Learning. Neuron *21*, 1399–1407. https://doi.org/10.1016/S0896-6273(00)80658-3.
13. Fuster, J.M., Bauer, R.H., and Jervey, J.P. (1982). Cellular discharge in the dorsolateral prefrontal cortex of the monkey in cognitive tasks. Exp. Neurol. *77*, 679–694. https://doi.org/10.1016/0014-4886(82)90238-2.
14. Rainer, G., Asaad, W.F., and Miller, E.K. (1998). Selective representation of relevant information by neurons in the primate prefrontal cortex. Nature *393*, 577–579. https://doi.org/10.1038/31235.

15. Miller, E.K., Erickson, C.A., and Desimone, R. (1996). Neural mechanisms of visual working memory in prefrontal cortex of the macaque. J. Neurosci. *16*, 5154–5167.

16. Romo, R., Brody, C.D., Hernández, A., and Lemus, L. (1999). Neuronal correlates of parametric working memory in the prefrontal cortex. Nature *399*, 470–473. https://doi.org/10.1038/20939.

17. Rigotti, M., Barak, O., Warden, M.R., Wang, X.J., Daw, N.D., Miller, E.K., and Fusi, S. (2013). The importance of mixed selectivity in complex cognitive tasks. Nature *497*, 585–590. https://doi.org/10.1038/nature12160.

18. Barraclough, D.J., Conroy, M.L., and Lee, D. (2004). Prefrontal cortex and decision making in a mixed-strategy game. Nat. Neurosci. *7*, 404–410. https://doi.org/10.1038/nn1209.

19. Seo, H., Barraclough, D.J., and Lee, D. (2007). Dynamic Signals Related to Choices and Outcomes in the Dorsolateral Prefrontal Cortex. Cerebr. Cortex *17*, i110–i117. https://doi.org/10.1093/cercor/bhm064.

20. Tsutsui, K.I., Grabenhorst, F., Kobayashi, S., and Schultz, W. (2016). A dynamic code for economic object valuation in prefrontal cortex neurons. Nat. Commun. *7*, 12554. https://doi.org/10.1038/ncomms12554.

21. Donahue, C.H., and Lee, D. (2015). Dynamic routing of task-relevant signals for decision making in dorsolateral prefrontal cortex. Nat. Neurosci. *18*, 295–301. https://doi.org/10.1038/nn.3918.

22. Olson, C.R., Musil, S.Y., and Goldberg, M.E. (1996). Single neurons in posterior cingulate cortex of behaving macaque: eye movement signals. J. Neurophysiol. *76*, 3285–3300.

23. Umeno, M.M., and Goldberg, M.E. (2001). Spatial Processing in the Monkey Frontal Eye Field. II. Memory Responses. J. Neurophysiol. *86*, 2344–2352. https://doi.org/10.1152/jn.2001.86.5.2344.

24. Tsujimoto, S., Genovesio, A., and Wise, S.P. (2009). Monkey orbitofrontal cortex encodes response choices near feedback time. J. Neurosci. *29*, 2569–2574. https://doi.org/10.1523/JNEUROSCI.5777-08.2009.

25. Tsujimoto, S., Genovesio, A., and Wise, S.P. (2010). Evaluating self-generated decisions in frontal pole cortex of monkeys. Nat. Neurosci. *13*, 120–126. https://doi.org/10.1038/nn.2453.

26. Bizzi, E. (1968). Discharge of frontal eye field neurons during saccadic and following eye movements in unanesthetized monkeys. Exp. Brain Res. *6*, 69–80. https://doi.org/10.1007/BF00235447.

27. Goldberg, M.E., and Bruce, C.J. (1990). Primate frontal eye fields. III. Maintenance of a spatially accurate saccade signal. J. Neurophysiol. *64*, 489–508. https://doi.org/10.1152/jn.1990.64.2.489.

28. Tsujimoto, S., and Sawaguchi, T. (2005). Context-dependent representation of response-outcome in monkey prefrontal neurons - PubMed. Cerebr. Cortex *15*, 888–898.

29. Tsujimoto, S., and Sawaguchi, T. (2004). Neuronal representation of response-outcome in the primate prefrontal cortex - PubMed. Cerebr. Cortex *14*, 47–55.

30. Funahashi, S. (2014). Saccade-related activity in the prefrontal cortex: its role in eye movement control and cognitive functions. Front. Integr. Neurosci. *8*, 54. https://doi.org/10.3389/fnint.2014.00054.

31. Xu, B.Y., Karachi, C., and Goldberg, M.E. (2012). The Postsaccadic Unreliability of Gain Fields Renders It Unlikely that the Motor System Can Use Them to Calculate Target Position in Space. Neuron *76*, 1201–1209. https://doi.org/10.1016/j.neuron.2012.10.034.

32. Khanna, S.B., Scott, J.A., and Smith, M.A. (2020). Dynamic shifts of visual and saccadic signals in prefrontal cortical regions 8Ar and FEF. J. Neurophysiol. *124*, 1774–1791. https://doi.org/10.1152/jn.00669.2019.

33. Kiani, R., Cueva, C.J., Reppas, J.B., Peixoto, D., Ryu, S.I., and Newsome, W.T. (2015). Natural Grouping of Neural Responses Reveals Spatially Segregated Clusters in Prearcuate Cortex. Neuron *85*, 1359–1373. https://doi.org/10.1016/j.neuron.2015.02.014.

34. Pasupathy, A., and Miller, E.K. (2005). Different time courses of learning-related activity in the prefrontal cortex and striatum. Nature *433*, 873–876. https://doi.org/10.1038/nature03287.

35. Law, C.-T., and Gold, J.I. (2008). Neural correlates of perceptual learning in a sensory-motor, but not a sensory, cortical area. Nat. Neurosci. *11*, 505–513.

36. Sommer, M.A., and Wurtz, R.H. (2000). Composition and topographic organization of signals sent from the frontal eye field to the superior colliculus. J. Neurophysiol. *83*, 1979–2001. https://doi.org/10.1152/jn.2000.83.4.1979.

37. Takeda, K., and Funahashi, S. (2002). Prefrontal Task-Related Activity Representing Visual Cue Location or Saccade Direction in Spatial Working Memory Tasks. J. Neurophysiol. *87*, 567–588. https://doi.org/10.1152/jn.00249.2001.

38. Bruce, C.J., Goldberg, M.E., Bushnell, M.C., and Stanton, G.B. (1985). Primate frontal eye fields. II. Physiological and anatomical correlates of electrically evoked eye movements. J. Neurophysiol. *54*, 714–734. https://doi.org/10.1152/jn.1985.54.3.714.

39. Funahashi, S., Chafee, M.V., and Goldman-Rakic, P.S. (1993). Prefrontal neuronal activity in rhesus monkeys performing a delayed anti-saccade task. Nature *365*, 753–756. https://doi.org/10.1038/365753A0.

40. Bullock, K.R., Pieper, F., Sachs, A.J., and Martinez-Trujillo, J.C. (2017). Visual and presaccadic activity in area 8Ar of the macaque monkey lateral prefrontal cortex. J. Neurophysiol. *118*, 15–28. https://doi.org/10.1152/jn.00278.2016.

41. Murray, J.D., Bernacchia, A., Roy, N.A., Constantinidis, C., Romo, R., and Wang, X.-J. (2017). Stable population coding for working memory coexists with heterogeneous neural dynamics in prefrontal cortex. Proc. Natl. Acad. Sci. USA *114*, 394–399. https://doi.org/10.1073/pnas.1619449114.

42. Cueva, C.J., Saez, A., Marcos, E., Genovesio, A., Jazayeri, M., Romo, R., Salzman, C.D., Shadlen, M.N., and Fusi, S. (2020). Low-dimensional dynamics for working memory and time encoding. Proc. Natl. Acad. Sci. USA *117*, 23021–23032. https://doi.org/10.1073/pnas.1915984117.

43. Khaki, M., LUNA, R., MORTAZAVI, N., SACHS, A., and MARTINEZ-TRUJILLO, J. (2021). Using classification-based decoding to analyze the Spatiotopic and Retinotopic memory representations in primates. J. Vis. *21*, 2868. https://doi.org/10.1167/JOV.21.9.2868.

44. Luna, R., Roussy, M.P., Corrigan, B., Sachs, A., Treue, S., and Martinez-Trujillo, J. (2021). Small neuronal ensembles of primate lateral prefrontal cortex encode spatial working memory in two reference frames. J. Vis. *21*, 2858. https://doi.org/10.1167/JOV.21.9.2858.

45. Luna Almeida, R., Roussy, M.P., Sachs, A., Treue, S., and Martinez-Trujillo, J.C. (2020). Neuronal ensembles of primate Lateral Prefrontal Cortex encode spatial working memory in different frames of reference. J. Vis. *20*, 1753. https://doi.org/10.1167/JOV.20.11.1753.

46. Stokes, M.G., Kusunoki, M., Sigala, N., Nili, H., Gaffan, D., and Duncan, J. (2013). Dynamic coding for cognitive control in prefrontal cortex. Neuron *78*, 364–375. https://doi.org/10.1016/j.neuron.2013.01.039.

47. Andersen, R.A., and Mountcastle, V.B. (1983). The influence of the angle of gaze upon the excitability of the light- sensitive neurons of the posterior parietal cortex. J. Neurosci. *3*, 532–548. https://doi.org/10.1523/JNEUROSCI.03-03-00532.1983.

48. Brotchie, P.R., Andersen, R.A., Snyder, L.H., and Goodman, S.J. (1995). Head position signals used by parietal neurons to encode locations of visual stimuli. Nature *375*, 232–235. https://doi.org/10.1038/375232a0.

49. Andersen, R.A., Essick, G.K., and Siegel, R.M. (1985). Encoding of spatial location by posterior parietal neurons. Science *230*, 456–458. https://doi.org/10.1126/science.4048942.

50. Andersen, R.A., Bracewell, R.M., Barash, S., Gnadt, J.W., and Fogassi, L. (1990). Eye position effects on visual, memory, and saccade-related activity in areas LIP and 7a of macaque. J. Neurosci. *10*, 1176–1196. https://doi.org/10.1523/JNEUROSCI.10-04-01176.1990.

51. Salinas, E., and Abbott, L.F. (2001). Chapter 11 Coordinate transformations in the visual system: how to generate gain fields and what to

compute with them. Prog. Brain Res. *130*, 175–190. https://doi.org/10.1016/S0079-6123(01)30012-2.

52. Meister, M.L.R., and Buffalo, E.A. (2018). Neurons in Primate Entorhinal Cortex Represent Gaze Position in Multiple Spatial Reference Frames. J. Neurosci. *38*, 2430–2441. https://doi.org/10.1523/JNEUROSCI.2432-17.2018.
53. Kim, S., Hwang, J., and Lee, D. (2008). Prefrontal Coding of Temporally Discounted Values during Intertemporal Choice. Neuron *59*, 161–172. https://doi.org/10.1016/j.neuron.2008.05.010.
54. Cohen, J.D., McClure, S.M., and Yu, A.J. (2007). Should I stay or should I go? How the human brain manages the trade-off between exploitation and exploration. Philos. Trans. R. Soc. Lond. B Biol. Sci. *362*, 933–942. https://doi.org/10.1098/rstb.2007.2098.
55. Domjan, M., and Grau, J.W. (2015). The Principles of Learning and Behavior (Cengage Learning).
56. Sugrue, L.P., Corrado, G.S., and Newsome, W.T. (2004). Matching behavior and the representation of value in the parietal cortex. Science (New York, N.Y.) *304*, 1782–1787. https://doi.org/10.1126/science.1094765.
57. Parthasarathy, A., Herikstad, R., Bong, J.H., Medina, F.S., Libedinsky, C., and Yen, S.C. (2017). Mixed selectivity morphs population codes in prefrontal cortex. Nat. Neurosci. *20*, 1770–1779. https://doi.org/10.1038/s41593-017-0003-2.
58. Spaak, E., Watanabe, K., Funahashi, S., and Stokes, M.G. (2017). Stable and dynamic coding for working memory in primate prefrontal cortex. J. Neurosci. *37*, 6503–6516. https://doi.org/10.1523/JNEUROSCI.3364-16.2017.
59. Raposo, D., Kaufman, M.T., and Churchland, A.K. (2014). A category-free neural population supports evolving demands during decision-making. Nat. Neurosci. *17*, 1784–1792. https://doi.org/10.1038/nn.3865.
60. Kim, J.-N., and Shadlen, M.N. (1999). Neural correlates of a decision in the dorsolateral prefrontal cortex of the macaque. Nat. Neurosci. *2*, 176–185. https://doi.org/10.1038/5739.
61. Kaufman, M.T., Benna, M.K., Rigotti, M., Stefanini, F., Fusi, S., and Churchland, A.K. (2022). The implications of categorical and category-free mixed selectivity on representational geometries. Curr. Opin. Neurobiol. *77*, 102644. https://doi.org/10.1016/J.CONB.2022.102644.
62. Tye, K.M., Miller, E.K., Taschbach, F.H., Benna, M.K., Rigotti, M., and Fusi, S. (2024). Mixed selectivity: Cellular computations for complexity. Neuron *112*, 2289–2303. https://doi.org/10.1016/J.NEURON.2024.04.017.
63. Petrides, M. (1985). Deficits in non-spatial conditional associative learning after periarcuate lesions in the monkey. Behav. Brain Res. *16*, 95–101.
64. Marmor, O., Pollak, Y., Doron, C., Helmchen, F., and Gilad, A. (2023). History information emerges in the cortex during learning. Elife *12*, e83702. https://doi.org/10.7554/ELIFE.83702.
65. Schall, J.D. (1997). Visuomotor Areas of the Frontal Lobe. Cerebr. Cortex *12*, 527–638. https://doi.org/10.1007/978-1-4757-9625-4_13.
66. Libby, A., and Buschman, T.J. (2021). Rotational dynamics reduce interference between sensory and memory representations. Nat. Neurosci. *24*, 715–726. https://doi.org/10.1038/s41593-021-00821-9.
67. Steel, A., Silson, E.H., Garcia, B.D., and Robertson, C.E. (2024). A retinotopic code structures the interaction between perception and memory systems. Nat. Neurosci. *27*, 339–347. https://doi.org/10.1038/s41593-023-01512-3.
68. Bizzi, E., and Schiller, P.H. (1970). Single unit activity in the frontal eye fields of unanesthetized monkeys during eye and head movement. Exp. Brain Res. *10*, 150–158. https://doi.org/10.1007/BF00234728.
69. Sendhilnathan, N., Basu, D., Goldberg, M.E., Schall, J.D., and Murthy, A. (2021). Neural correlates of goal-directed and non-goal-directed movements. Proc. Natl. Acad. Sci. USA *118*, 2021. https://doi.org/10.1073/PNAS.2006372118/SUPPL_FILE/PNAS.2006372118.SAPP.PDF.
70. Histed, M.H., Pasupathy, A., and Miller, E.K. (2009). Learning Substrates in the Primate Prefrontal Cortex and Striatum: Sustained Activity Related to Successful Actions. Neuron *63*, 244–253. https://doi.org/10.1016/j.neuron.2009.06.019.
71. Kiani, R., Cueva, C.J., Reppas, J.B., and Newsome, W.T. (2014). Dynamics of Neural Population Responses in Prefrontal Cortex Indicate Changes of Mind on Single Trials. Curr. Biol. *24*, 1542–1547. https://doi.org/10.1016/J.CUB.2014.05.049.
72. Purcell, B.A., and Kiani, R. (2016). Neural Mechanisms of Post-error Adjustments of Decision Policy in Parietal Cortex. Neuron *89*, 658–671. https://doi.org/10.1016/j.neuron.2015.12.027.
73. Rabbitt, P., and Rodgers, B. (1977). What does a man do after he makes an error? an analysis of response programming. Q. J. Exp. Psychol. *29*, 727–743.
74. Massi, B., Donahue, C.H., and Lee, D. (2018). Volatility Facilitates Value Updating in the Prefrontal Cortex. Neuron *99*, 598–608. https://doi.org/10.1016/J.NEURON.2018.06.033.
75. Fu, Z., Beam, D., Chung, J.M., Reed, C.M., Mamelak, A.N., Adolphs, R., and Rutishauser, U. (2022). The geometry of domain-general performance monitoring in the human medial frontal cortex. Science *376*, eabm9922. https://doi.org/10.1126/SCIENCE.ABM9922/SUPPL_FILE/SCIENCE.ABM9922_MDAR_REPRODUCIBILITY_CHECKLIST.PDF.
76. Cortes, C., Vapnik, V., and Saitta, L. (1995). Support-Vector Networks Editor. Machine Leaming *20*, 273–297.
77. Hennig, J., Oby, E.R., Losey, D.M., Batista, A.P., Yu, B.M., and Chase, S.M. (2021). How learning unfolds in the brain: toward an optimization view. Neuron *109*, 3720–3735.
78. Wang, J.X., Kurth-Nelson, Z., Kumaran, D., Tirumala, D., Soyer, H., Leibo, J.Z., Hassabis, D., and Botvinick, M. (2018). Prefrontal cortex as a meta-reinforcement learning system. Nat. Neurosci. *21*, 860–868. https://doi.org/10.1038/s41593-018-0147-8.
79. Curtis, C.E., and Lee, D. (2010). Beyond working memory: The role of persistent activity in decision making. Trends Cognit. Sci. *14*, 216–222. https://doi.org/10.1016/j.tics.2010.03.006.
80. Tsujimoto, S., Genovesio, A., and Wise, S.P. (2011). Frontal pole cortex: Encoding ends at the end of the endbrain. Trends Cognit. Sci. *15*, 169–176. https://doi.org/10.1016/J.TICS.2011.02.001.
81. Compte, A., Brunel, N., Goldman-Rakic, P.S., and Wang, X.J. (2000). Synaptic Mechanisms and Network Dynamics Underlying Spatial Working Memory in a Cortical Network Model. Cerebr. Cortex *10*, 910–923. https://doi.org/10.1093/CERCOR/10.9.910.
82. Barbosa, J., Stein, H., Martinez, R.L., Galan-Gadea, A., Li, S., Dalmau, J., Adam, K.C.S., Valls-Solé, J., Constantinidis, C., and Compte, A. (2020). Interplay between persistent activity and activity-silent dynamics in the prefrontal cortex underlies serial biases in working memory. Nat. Neurosci. *23*, 1016–1024. https://doi.org/10.1038/s41593-020-0644-4.
83. Koechlin, E. (2016). Prefrontal executive function and adaptive behavior in complex environments. Curr. Opin. Neurobiol. *37*, 1–6. https://doi.org/10.1016/J.CONB.2015.11.004.
84. Averbeck, B., and O'Doherty, J.P. (2021). Reinforcement-learning in fronto-striatal circuits. Neuropsychopharmacology *47*, 147–162. https://doi.org/10.1038/s41386-021-01108-0.
85. Lee, D., Seo, H., and Jung, M.W. (2012). Neural Basis of Reinforcement Learning and Decision Making. Annu. Rev. Neurosci. *35*, 287–308. https://doi.org/10.1146/ANNUREV-NEURO-062111-150512.
86. Lee, D., and Seo, H. (2007). Mechanisms of Reinforcement Learning and Decision Making in the Primate Dorsolateral Prefrontal Cortex. Ann. N. Y. Acad. Sci. *1104*, 108–122. https://doi.org/10.1196/ANNALS.1390.007.
87. Lim, D.H., Yoon, Y.J., Her, E., Huh, S., and Jung, M.W. (2020). Active maintenance of eligibility trace in rodent prefrontal cortex. Sci. Rep. *10*, 18860. https://doi.org/10.1038/s41598-020-75820-0.
88. Parker, N.F., Baidya, A., Cox, J., Haetzel, L.M., Zhukovskaya, A., Murugan, M., Engelhard, B., Goldman, M.S., and Witten, I.B. (2022).

Choice-selective sequences dominate in cortical relative to thalamic inputs to NAc to support reinforcement learning. Cell Rep. *39*, 110756. https://doi.org/10.1016/J.CELREP.2022.110756.

89. Harvey, C.D., Coen, P., and Tank, D.W. (2012). Choice-specific sequences in parietal cortex during a virtual-navigation decision task. Nature *484*, 62–68. https://doi.org/10.1038/nature10918.
90. Koay, S.A., Charles, A.S., Thiberge, S.Y., Brody, C.D., and Tank, D.W. (2022). Sequential and efficient neural-population coding of complex task information. Neuron *110*, 328–349.e11. https://doi.org/10.1016/J.NEURON.2021.10.020.
91. Bichot, N.P., Schall, J.D., and Thompson, K.G. (1996). Visual feature selectivity in frontal eye fields induced by experience in mature macaques. Nature *381*, 697–699. https://doi.org/10.1038/381697a0.
92. White, I.M., and Wise, S.P. (1999). Rule-dependent neuronal activity in the prefrontal cortex. Exp. Brain Res. *126*, 315–335. https://doi.org/10.1007/s002210050740.
93. Yang, G.R., Joglekar, M.R., Song, H.F., Newsome, W.T., and Wang, X.J. (2019). Task representations in neural networks trained to perform many cognitive tasks. Nat. Neurosci. *22*, 297–306. https://doi.org/10.1038/s41593-018-0310-2.
94. Kirkpatrick, J., Pascanu, R., Rabinowitz, N., Veness, J., Desjardins, G., Rusu, A.A., Milan, K., Quan, J., Ramalho, T., Grabska-Barwinska, A., et al. (2017). Overcoming catastrophic forgetting in neural networks. Proc. Natl. Acad. Sci. USA *114*, 3521–3526. https://doi.org/10.1073/pnas.1611835114.
95. Sommer, M.A., and Wurtz, R.H. (2008). Visual perception and corollary discharge. Perception *37*, 408–418. https://doi.org/10.1068/p5873.
96. Sommer, M.A., and Wurtz, R.H. (2008). Brain circuits for the internal monitoring of movements. Annu. Rev. Neurosci. *31*, 317–338. https://doi.org/10.1146/ANNUREV.NEURO.31.060407.125627.
97. Neupane, S., Guitton, D., and Pack, C.C. (2016). Two distinct types of remapping in primate cortical area V4. Nat. Commun. *7*, 10402. https://doi.org/10.1038/ncomms10402.
98. Duhamel, J.R., Colby, C.L., and Goldberg, M.E. (1992). The updating of the representation of visual space in parietal cortex by intended eye movements. Science (New York, N.Y.) *255*, 90–92. https://doi.org/10.1126/science.1553535.
99. Marino, A.C., and Mazer, J.A. (2016). Perisaccadic Updating of Visual Representations and Attentional States: Linking Behavior and Neurophysiology. Frontiers *10*, 3.
100. Marino, A.C., and Mazer, J.A. (2018). Saccades Trigger Predictive Updating of Attentional Topography in Area V4. Neuron *98*, 429–438. https://doi.org/10.1016/J.NEURON.2018.03.020.
101. Mays, L.E., and Sparks, D.L. (1980). Dissociation of visual and saccade-related responses in superior colliculus neurons - PubMed. J. Neurophysiol. *43*, 207–232.
102. Wurtz, R.H. (2018). Corollary Discharge Contributions to Perceptual Continuity Across Saccades. Annual review of vision science, 215–237. https://doi.org/10.1146/ANNUREV-VISION-102016-061207.
103. Alexander, W.H., and Brown, J.W. (2011). Medial prefrontal cortex as an action-outcome predictor. Nat. Neurosci. *14*, 1338–1344. https://doi.org/10.1038/nn.2921.
104. Heinzle, J., Aponte, E.A., and Stephan, K.E. (2016). Computational models of eye movements and their application to schizophrenia. Current Opinion in Behavioral Sciences *11*, 21–29. https://doi.org/10.1016/J.COBEHA.2016.03.008.
105. Adámek, P., Langová, V., and Horáček, J. (2022). Early-stage visual perception impairment in schizophrenia, bottom-up and back again. Schizophrenia *8*, 1–12. https://doi.org/10.1038/s41537-022-00237-9.
106. Broerse, A., Crawford, T.J., and Den Boer, J.A. (2001). Parsing cognition in schizophrenia using saccadic eye movements: a selective overview. Neuropsychologia *39*, 742–756. https://doi.org/10.1016/S0028-3932(00)00155-X.
107. Egaña, J.I., Devia, C., Mayol, R., Parrini, J., Orellana, G., Ruiz, A., and Maldonado, P.E. (2013). Small saccades and image complexity during free viewing of natural images in schizophrenia. Front. Psychiatr. *4*, 37. https://doi.org/10.3389/FPSYT.2013.00037/BIBTEX.
108. Sutton, R.S., Barto, A.G., and Book, A.B. (2017). Reinforcement Learning: An Introduction (MIT press).
109. Gnadt, J.W., and Andersen, R.A. (1988). Memory related motor planning activity in posterior parietal cortex of macaque. Exp. Brain Res. *70*, 216–220. https://doi.org/10.1007/BF00271862.
110. Ding, L., and Gold, J.I. (2010). Caudate encodes multiple computations for perceptual decisions. J. Neurosci. *30*, 15747–15759. https://doi.org/10.1523/JNEUROSCI.2894-10.2010.
111. Evarts, E.V. (1966). Pyramidal tract activity associated with a conditioned hand movement in the monkey. J. Neurophysiol. *29*, 1011–1027. https://doi.org/10.1152/JN.1966.29.6.1011.
112. Judge, S.J., Richmond, B.J., and Chu, F.C. (1980). Implantation of magnetic search coils for measurement of eye position: an improved method. Vis. Res. *20*, 535–538. https://doi.org/10.1016/0042-6989(80)90128-5.
113. Suner, S., Fellows, M.R., Vargas-Irwin, C., Nakata, G.K., and Donoghue, J.P. (2005). Reliability of Signals From a Chronically Implanted, Silicon-Based Electrode Array in Non-Human Primate Primary Motor Cortex. IEEE Trans. Neural Syst. Rehabil. Eng. *13*, 524–541. https://doi.org/10.1109/TNSRE.2005.857687.
114. Santhanam, G., Ryu, S.I., Yu, B.M., Afshar, A., and Shenoy, K.V. (2006). A high-performance brain–computer interface. Nature *442*, 195–198. https://doi.org/10.1038/nature04968.
115. Mould, M.S., Foster, D.H., Amano, K., and Oakley, J.P. (2012). A simple nonparametric method for classifying eye fixations. Vis. Res. *57*, 18–25. https://doi.org/10.1016/j.visres.2011.12.006.
116. Graf, A.B.A., Kohn, A., Jazayeri, M., and Movshon, J.A. (2011). Decoding the activity of neuronal populations in macaque primary visual cortex. Nat. Neurosci. *14*, 239–245. https://doi.org/10.1038/nn.2733.

## STAR★METHODS

### KEY RESOURCES TABLE

| REAGENT or RESOURCE | SOURCE | IDENTIFIER |
|---|---|---|
| Deposited data | | |
| Neural Data | Zenodo | https://doi.org/10.5281/zenodo.14360532 |
| Experimental models: Organisms/Strains | | |
| Rhesus macaque (Macaca mulatta) | – | N/A |
| Software and algorithms | | |
| MATLAB | Mathworks | https://mathworks.com/ |
| Plexon Offline Sorter | Plexon | https://plexon.com/ |
| REX software environment and QNX Software System's | Ottawa, Canada | https://www.qnx.com/ |
| Other | | |
| scleral eye coils | C-N-C Engineering, Seattle, WA | https://www.sr-research.com/eyelink-1000-plus/ |
| VSG graphics card | Cambridge Graphics, UK | https://www.crsltd.com/tools-for-vision-science |

### EXPERIMENTAL MODEL AND SUBJECT DETAILS

We collected behavioral and neural data from three adult male rhesus monkeys: monkeys T (14 kg), V (11 kg) and C (13 kg). All three monkeys were adult monkeys. All surgical, behavioral, and animal-care procedures complied with National Institutes of Health guidelines and were approved by the Stanford University Institutional Animal Care and Use Committee. Prior to training, the monkeys were implanted with a stainless-steel head holder[111] and a scleral search coil for monitoring monocular eye position.[112] We used operant conditioning with liquid rewards to train the monkeys to perform a visually guided, delayed-saccade task; a two-alternative, forced-choice, motion discrimination task; and a two-alternative, forced-choice, non-spatial associative task. During training and experimental sessions, monkeys sat in a primate chair with their head restrained. Visual stimuli were presented on a cathode ray tube monitor controlled by a VSG graphics card (Cambridge Graphics, UK), at a frame rate of 120Hz, and viewed from a distance of 57 cm. Eye movements were monitored through the scleral eye coils (C-N-C Engineering, Seattle, WA). Behavioral control and data acquisition were managed by a computer running the REX software environment and QNX Software System's (Ottawa, Canada) real-time operating system.

### METHOD DETAILS

#### Behavioral tasks

##### *Instructed saccade task*

Monkeys were engaged in a visually-guided, delayed-saccade task, requiring them to perform a sequence of saccades and fixations on each trial to obtain a reward (Figure 1A). A trial was initiated by a saccade to the fixation point, and subsequently the monkey was required to maintain fixation until the offset of the fixation point. At 0.6–0.8s after fixation onset, a saccade target was presented in the periphery (33 unique positions per experiment for monkey T and 24 for monkey V and C). The fixation cue disappeared after an interval of random duration following the target onset (0.7–1.2s) instructing the monkey to execute the saccade to the target. After the saccade, the monkey was again required to maintain fixation, this time on the target, for the duration of another random time interval (0.8–1.5s). At the end of this interval, the target disappeared, a reward was delivered, and the monkey was free to move the eyes. The three randomized intervals were drawn from uniform distribution.

Note that for monkey T possible targets were placed 30° apart, but only 11 out of 12 ({0,30,60,90,120,150,180,210,240,270,300,330} degrees) directions were used per experiment. Specifically, targets at 120° were never present in 5 sessions; 300° never appeared in 3 sessions and 210° never appeared in one session. Each target direction could appear at one of three eccentricities or radii ({4,8,12}). For monkey V and monkey C, each recording session included 24 unique target locations (8 target directions placed at 45° apart and 3 possible radii - 4, 8 and 12).

For the instructed saccade task, we analyzed neural recordings obtained when the monkeys were proficient at the task, i.e., there are no error trials and the direction of the rewarded saccade always refers to the target location. We analyzed a total of 9/10/10 experiments with 20,952/4751/8611 trials and 1706/2334/2095 single and multi-units from the three arrays in monkeys T/V/C.

### *Perceptual decision-making task (moving-dots)*

Monkeys were engaged in a two-alternative, forced-choice motion discrimination task (Figures 2D and 2E). The timing of task events was similar to the instructed saccade task (i.e., it included the random interval of target-fixation after the choice saccade). On each trial monkeys observed a noisy, random-dots motion stimulus presented through a circular aperture and had to report the prevalent direction of motion with a saccade toward one of two visual targets. Correct choices (e.g., a saccade to the right target for predominant rightward motion) were rewarded at the end of the target-fixation period. The strength of the motion stimulus (motion coherence) was set pseudo-randomly on each trial. For low motion coherences, the monkeys' performance was close to chance level (50%), while for high coherences it was close to perfect (not shown). In this manuscript we only analyzed rewarded trials with high motion coherence stimulus.

### *Shifted workspace for the perceptual task*

We used a modified version of the moving-dots task to investigate whether post-saccadic activity of the rewarded saccade is affected by the position of the eye (Figure 2D). The timing of relevant task-events was analogous to that in the instructed saccade task, and included a target-fixation-period after the rewarded saccade (i.e., the choice saccade). Critically, each experiment in this task included trials from two "shifted" workspaces, whereby the location of the fixation point was shifted to the left from the midline in one workspace (relative to head-position), and to the right in the other (Figure 2D, "left" and "right" workspaces). As a result, saccade direction and gaze-location of the rewarded saccade are somewhat decoupled—for example, the location corresponding to the center of the monitor could either be the target of a rightward or a leftward saccade (Figure 2D, left vs. right workspace).

### *Associative task*

Monkeys were engaged in a two-alternative, forced-choice task that required them to track which of two targets (red or green) was being rewarded at any given time (Figure 6A). Throughout the day, the reward contingencies switched repeatedly between two "contexts": in the red context, only saccades to the red target were rewarded, and in the green context only saccades to the green target were rewarded. Because the timing of switches in reward contingencies was unpredictable, the optimal strategy is "win-stay-lose-switch": if a given color was rewarded ("win"), the monkey should choose the same color again in the next trial ("stay"). Instead, after a choice that was not rewarded ("lose") the monkeys should switch to the other color ("switch").

This task that had the same trial structure as the instructed saccade task, namely a central-fixation period of random duration between targets appearance, and the saccade (choice-saccade) toward one of them; followed by a target-fixation period of random duration requiring monkeys to fixate the chosen target until feedback.

### *Same recording day for perceptual task, instructed saccade and associative with 2 targets*

On some recording days, monkey T (12 sessions) and monkey V (2 sessions) performed three tasks sequentially: the perceptual task (random-dots), the instructed saccade task where one target could appear in one of two locations and the non-spatial associative task (Figure 3). Importantly, the target locations across the three tasks were identical, allowing the comparison of saccade-related activity across the different tasks.

## Neurophysiological recording

We recorded single and multi-unit neural signals with a chronically-implanted 10 by 10 array of electrodes (Cyberkinetics Neurotechnology Systems, Foxborough, MA; now Blackrock Microsystems). The inter-electrode spacing was 0.4 mm; electrodes were 1.5 mm long. Arrays were surgically implanted into the pre-arcuate gyrus[113,114] We targeted the array to a region of prefrontal cortex between the posterior end of the principal sulcus, and the anterior bank of the arcuate sulcus, near the rostral zone of Brodmann's area 8 (area 8Ar) in monkeys T and V. The arrays were implanted in the left hemisphere in both monkeys. The exact location of the array varied slightly across the two monkeys (Figure S1A), due to inter-animal variations in cortical vasculature and sulcal geometry that constrained the location of the array insertion site. In monkey C the array was placed between the superior branch of arcuate sulcus and dorsal bank of the principal sulcus, in the right hemisphere.

Array signals were amplified with respect to a common subdural ground, filtered and digitized using hardware and software from Cyberkinetics. For each of the 96 recording channels, 'spikes' from the entire duration of a recording session were sorted and clustered offline, based on a principal component analysis of voltage waveforms, using Plexon Offline Sorter (Plexon Inc., Dallas, Texas). This automated process returned a set of candidate action-potential classifications for each electrode that were subject to additional quality controls, including considerations of waveform shape, waveform reproducibility, inter-spike interval statistics, and the overall firing rate. For clusters returned by this postprocessing, both spike-waveform and spike-timing metrics fell within previously reported ranges for array recordings.[113]

Daily recordings yielded 100–200 single and multi-unit clusters distributed across the array. We do not differentiate between single-unit and multi-unit recordings, referring to both collectively as 'units'. Therefore, we also do not draw conclusions in this study that depend on the distinction between single and multi-unit responses. Neural responses in the instructed saccade task were recorded over a total of 9, 10, 10 experiments in monkeys monkey T, monkey V and monkey C, for a total of 20,905, 4751 and 8611 trials.

## QUANTIFICATION AND STATISTICAL ANALYSES

### Analysis of eye movement data

#### *Saccade extraction*

We used a non-parametric data-driven method for classifying eye fixations and saccades that automatically adapts itself to the task statistics.[115] The method is built on the assumption that the eye reaches higher speeds during saccades than during fixations, and that there are fewer peaks in speed due to saccades than due to fixations. Using these observations about the statistics of eyebehavior, the method derives an optimum speed threshold that best separates the speed distribution of saccades from the speed distribution of fixations and instrumental noise.

#### *Saccade types*

We analyze neural activity related to different types of saccades, i.e., the instructed and freely initiated saccades occurring before, during, and after each trial (Figures 1B and 1C). We refer to the initial saccade to the fixation point as the start saccade, the saccade to the target as the rewarded saccade, and the saccade away from the target after reward delivery as the end saccade. The start saccade is therefore visually-guided and non-rewarded; the rewarded saccade is visually-guided and rewarded; and the end saccade is free and non-rewarded. Monkeys initiate the end saccade when there is nothing on the screen. The saccade durations are 54ms (95% CI 52, 55), 37ms (95% CI 36, 38) and 140ms (95% CI 125, 154) for monkey T, for the start, rewarded and end saccades respectively.

In the instructed saccade task, in approximately 45% (monkey T) and 33% (monkey V) trials the monkeys were already at fixation point when the new trial started, thus there are fewer start saccades than end saccades.

### Analysis of behavioral data in the non-spatial associative task

We characterized fast learning with logistic regression models fit to the behavior in a single session. We separately modeled the influence of the (task relevant) target color and the (task irrelevant) target location on the monkeys' choices (Figure 6C, circles and squares) and their interaction with previous outcome (win or lose, x- and y axes).

$$\text{logit } p(\text{stay}_k) = \beta_0 + \beta_1 r_{k-1}$$

where logit $p(\text{stay}_k)$ denotes the probability of choosing on trial k the same choice (same color for the optimal strategy and same location for the suboptimal) as in the previous trial k-1 and $r_{k-1}$ is 1 when the outcome of the previous trial was a reward and 0 when it was not rewarded.

$$\text{logit } p(\text{stay}_k) = \begin{cases} \beta_0 + \beta_1, \text{if } r_{k-1} = 1 \text{ (post } - \text{ win)} \\ \beta_0, \text{if } r_{k-1} = 0 \text{ (post } - \text{ lose)} \end{cases}$$

Then, we compute logit $p(\text{stay}_k)$ in post-win trials:

$$\text{logit } p(\text{win-stay}_k) = \beta_0 + \beta_1$$

and logit $p(\text{switch}_k)$ in post-lose trials:

$$\text{logit } p(\text{lose-switch}_k) = 1 - \beta_0$$

In Figure 6C we subtract from these probabilities the estimated probabilities of random behavior and obtain $\Delta P(\text{lose} - \text{switch})$ and $\Delta P(\text{win} - \text{stay})$. For the optimal model (color), we simulate random colour-choices. Fitting the logistic regression to these random colour-choices, i.e., the colour-choice on trial k is independent from the colour-choice on trial k-1:

$$\text{logit } p(\text{stay}_k) = \beta_0 + \beta_1 r_{k-1}$$

we estimate $p(\text{win-stay}^{\text{color}})_{\text{random}} = 0.5$ and $p(\text{lose-switch}^{\text{color}})_{\text{random}} = 0.5$. Then, for the colour-model,

$$\Delta P\left(\text{win-stay}^{\text{color}}\right) = p\left(\text{win-stay}^{\text{color}}\right) - p\left(\text{win-stay}^{\text{color}}\right)_{\text{random}}$$

$$\Delta P\left(\text{lose-switch}^{\text{color}}\right) = p\left(\text{lose-switch}^{\text{color}}\right) - p\left(\text{lose-switch}^{\text{color}}\right)_{\text{random}}$$

The relation between space and color was pseudo-randomized in some sessions and this resulting deviation from perfect randomness lead to apparent biases in the behavior that we seek to remove. Using such relative probabilities allowed us to compensate for any potential biases in choices due to lack of complete randomization (e.g., because of the limited number of switches in a trial, and the fact that timing of transitions is pseudo-randomized, rather than being completely random). Therefore, for the location-model, we corrected the estimated probabilities of the monkey's behavior by (1) using their observed colour-choices; (2) converting the colour-choice into a location-choice, based on the experimentally-set colour-location association of each trial; (3) estimating $p(\text{win-stay}^{\text{location}})_{\text{random}}$ and $p(\text{lose-switch}^{\text{location}})_{\text{random}}$.

### *Linking neural and behavioral data*

We studied how slow learning shapes the neural responses by correlating timespecific decoding accuracies with different behavioral variables. Notably, we used partial correlation to remove modulations due to target configuration (Figures S9C and S9D). Target configuration was included through one-hot encoding. Behavioral variables we considered are: training day, first half vs. second half training day (1 for first half and 2 for second half) and the modeled probabilities of the task relevant model. The results were quantitively similar. The *p*-values in Figures 7B and S9B are for the partial correlation with first half vs. second half training day. P-value is computed as the number of shuffled partial correlations that exceed the empirical partial correlation. Shuffled partial correlations were computed by correlating behavioral variable to 1000 random permutations of decoding accuracies.

## Task epochs used for analysis of neural data

Throughout the paper, we consider neural responses occurring during four distinct, largely non-overlapping trial epochs. We refer to the first randomized time interval, following the start saccade, as the first central-fixation-period (i.e., fixation on the fixation point, 0.6–0.8s); the second randomized interval, preceding the rewarded saccade, as the second central-fixation-period (0.7–1.2s); and the last randomized interval, preceding the reward, as the target-fixationperiod (i.e., fixation on the target, 0.8–1.5s). Lastly, we analyze the times around the end saccade, whose onset is after reward delivery. Notably, the onset of the end saccade does not coincide with the time of reward delivery on every single trial - on some trials monkeys initiate the end-saccade immediately after reward and on some trials monkeys continue fixating the location where the target was present, on a few trials for intervals as long as 600ms.

## Analysis of single-unit responses

### *Pre-processing condition-averaged responses*

We bin activity in 50ms non-overlapping bins and we normalize the unit responses using z-scoring:

$$z_{i,t}(l) = \frac{z^{\text{raw}}_{i,t}(l) - \langle z^{\text{raw}}_{i,t}(l)\rangle_{t,l}}{std\left(z^{\text{raw}}_{i,t}(l)\right)_{t,l} + \overline{\sigma}}$$

where $z^{\text{raw}}_{i,t}(l)$ and $z_{i,t}(l)$ are the raw firing rate and z-scored responses, respectively, of unit $i$ at time $t$ and on trial $l$, $\langle\cdot\rangle_{t,l}$ and $std_{t,l}$ indicate the mean and standard deviation across times and trials, and $\overline{\sigma}$ is a constant defined as the median of the standard deviation across all units in a session. The z-scoring de-emphasizes the contribution to the population responses of units with very high firing rates (typically multi-unit activity), while the constant term ensures that units with very small firing rates are not over-emphasized. The for unit-level analysis, we do not apply any other temporal smoothing to the responses.

We defined condition-averaged responses $f_{i,t,c}$ for each unit by averaging the normalized time-varying firing rates across all trials belonging to a given condition *'c'* (Figure 4A). For the instructed saccade task, we define each condition by the saccade direction (11 conditions for monkey T, 8 conditions for monkey V and monkey C).

The condition-averaged responses were de-noised using Singular Vector Decomposition (SVD). We concatenated the condition-averaged responses $f_{i,t,\theta}$ across all recording sessions with the same conditions in a $N_{unit} \times (N_{condition} \cdot T)$ matrix, where $N_{unit}$ is the total number of units, $N_{condition}$ is the total number of conditions, and $T$ is the number of bins. The left singular-vectors of this data matrix are vectors $\boldsymbol{v}_a$ of length $N_{unit}$, indexed by $a$, ordered from the singular-vector explaining the most variance to the one explaining the least. We use the first $N_{svd}$ singular-vectors to define a de-noising matrix $\boldsymbol{D}$ of size $N_{unit} \times N_{unit}$:

$$\boldsymbol{D} = \sum_{a=1}^{N_{svd}} \boldsymbol{v}_a \boldsymbol{v}_a^T$$

We used this matrix to de-noise the condition-averaged responses by projecting them into the sub-space spanned by the first $N_{svd}$ singular-vectors:

$$f^{svd}_{i,t,\theta} = \boldsymbol{D} f_{i,t,\theta}$$

We use the de-noised condition-averaged responses $f^{svd}_{i,t,\theta}$ to determine the unit-specific optimal direction, i.e., the condition that elicits the highest responses. From now on $f_{i,t,\theta}$ will refer to the de-noised responses.

### *Bell-shaped model of direction selectivity*

We estimated, for each unit, the saccade-location that elicits the highest response at each time by fitting a descriptive function[11] to the normalized time varying condition-averaged responses (Figure 4B):

$$g(\theta) = baseline_\theta + gain_\theta * \exp\left(-\frac{(\theta - \theta_0)^2}{2\sigma_\theta^2}\right)$$

where $\theta_0$ is the preferred saccade direction, $\sigma_\theta$ determines the tuning width and $gain_\theta$ determines the modulation depth of the tuning curve.

We fitted the parameters of these models separately for each unit to averaged responses grouped by saccade-direction within the epoch [0, 0.7]s after target onset and [-0.3, 0.5]s around saccade initiation, in 50ms non-overlapping bins. The models are fit by minimizing the summed square error across the respective conditions between the model predictions and the corresponding condition-averaged response.

### *Goodness-of-fit*

We validated the 1-D Gaussian models by computing a coefficient of determination ($R^2$) (Figure 4B) value from the measured condition-averaged response $f_{i,t,\theta}$ and the model's reconstruction $\widehat{f_{i,t,\theta}}$, based on comparing the variability of the estimation errors with the variability of the original neural responses.

$$r^2_{i,t,\theta} = \max\left(0, 1 - \frac{\sum_{\theta}\|f_{i,t,\theta} - \widehat{f_{i,t,\theta}}\|^2}{\sum_{\theta}\left(f_{i,t,\theta} - \langle f_{i,t,\theta}\rangle_{\theta}\right)^2}\right)$$

Model parameters were found from condition-averages computed on a subset of trials (training set) and validated on condition-averages computed on a different, non-overlapping subset of trials (testing set). All units that had a coefficient of determination different than 0 were considered selective (Figure 4C, top row). A coefficient of determination equal to 0 indicates that the condition-averaged response is better described by the averaged response across all conditions $\langle f_{i,t,\theta}\rangle_{\theta}$.

### *Cross-temporal selectivity measure*

We quantified the percentage of selective units at different time-pairs ($t_m$,$t_n$) (Figure 4C, bottom row):

$$n_{(t_m,\,t_n)} = \sum_k \begin{cases} 1; & \text{if } r^2_{i,t_m,\theta} > 0 \text{ and } r^2_{i,t_n,\theta} > 0 \\ 0; & \text{otherwise} \end{cases}$$

where i is unit index.

To assess the significance of each $n_{(t_m,\,t_n)}$, we shuffled the unit-order independently at $t_m$ and $t_n$ and re-computed the number of units that were selective at both times. We repeated this procedure 1000 times and compared the measured $n_{(t_m,\,t_n)}$ to the 95th percentile of this distribution.

## Decoding analysis of population responses

For the population-level analysis, we compute binned spike counts in 100ms overlapping bins. Chance level of decoding analyses is computed using 11 classes (9%) for monkey T and 8 classes (12.5%) for monkey V and monkey C. We quantified the relation between single-trial normalized population responses and the saccade direction using high-dimensional decoders suited for multi-class problems (Figures 1D and 1E for monkey T; Figures S3B and S3G for monkey V and C). To ensure our results do not depend on the choice of the decoder, we used several types of decoders (Figure S2E for monkey T; Figures S3E and S2J for monkey V and C). Specifically, we used MATLAB built-in classifiers: Linear discriminant analysis (fitcdiscr), Naive Bayes (fitcnb) and Error-correcting SVM (fitcecoc), as well as a customized classifier (Circular-SVM).

### *Circular-SVM*

This previously proposed method[116] builds on the Naive Bayes model. Knowing that the topography of the neural responses is circular, it learns the pooling weight **W**, i.e., how each unit influences the classifier's prediction, in a model-free way, directly from the neural data. We describe the method briefly, for more details see.[116]

Discrimination between two saccade directions $\theta_1$ and $\theta_2$ is done using the sign of the Support-Vector Machine (SVM) decision function:

$$y(\theta_1,\theta_2) = \sum_{i=1}^{N_{unit}} w_i(\theta_1,\theta_2)x_i + b(\theta_1,\theta_2) \equiv \log LR(\theta_1,\theta_2)$$

$$\log LR(\theta_1,\theta_2) = \log\frac{L(\theta_1)}{L(\theta_2)} = \log L(\theta_1) - \log L(\theta_2) = \sum_{i=1}^{N_{unit}} [W_i(\theta_1) - W_i(\theta_2)]r_i + [B(\theta_1) - B(\theta_2)] = \sum_{i=1}^{N_{unit}} w_i(\theta_1,\theta_2)x_i + b(\theta_1,\theta_2)$$

The SVM decision function is used as a local linear approximation of the difference between the log likelihood evaluated at two saccade directions. The entire log likelihood function is reconstructed by computing the cumulative sum of the empirical log likelihood ratios of adjacent directions:

$$logL(\theta_j) = \sum_{k=2}^{j} logLR(\theta_k,\theta_{k-1}) = \sum_{i=1}^{N_{unit}} W_i(\theta_j)r_j + B(\theta_j)$$

with $\log(\theta_1) = 0$.

Some pairs of neighboring directions are better separated than others. We modified the original version of the method such that the discriminability of a saccade-direction would only depend on how well it is separated from its two immediate neighboring directions,

and not on how well separated are any other two neighboring directions. To compute an unbiased log likelihood, each angle $\theta_j$ takes turn in being the reference $\log(\theta_j) = 0$. In this manner, we average out the cumulated-error.

***Decoding variable (saccade direction)***

For the **rewarded saccade**, we study the relationship between the population responses and saccade direction through cross-validated high-dimensional decoders (Figure 1D for monkey T; Figures S3B and S3G for monkey V and C). For the **start** and **end saccade**, we apply the same decoders we identified for the rewarded saccade to responses aligned to the start and end saccade (Figure 1E for monkey T; Figures S3C and S3H for monkey V and C). Training a new set of decoders on responses aligned to the end saccade resulted on similar crossvalidated accuracies when used to readout the end saccade (results not shown).

***Time-specific decoding***

Decoders are trained and tested on time-specific responses using 10-fold crossvalidation.

***Cross-temporal decoding***

Decoders are tested on responses outside their training time-window (Figure 3D). A decoding matrix $T \times T$ contains the cross-validated decoding accuracy of T time-specific decoders tested on T time-specific population-responses. The diagonal of this decoding matrix is the time-specific decoding accuracy. All decoders are cross-validated, i.e., that even though the decoders are trained at one time and tested at another time, there is no overlap between the train and test trials. This analysis shows how each of the time-specific mappings generalize across responses at other times in the trial.

## Post-saccadic activity is not pre-saccadic activity for the next saccade

One possible interpretation of post-saccadic activity is that it encodes the planning of the next saccade (Figures 2A–2C). To test this hypothesis, we decoded the direction of the end saccade from activity preceding the end saccade and from activity during the target-fixation-period (Figure 2B). Ruling out this hypothesis is very challenging because the behavior of the monkeys is biased - very often the end saccade is back to the fixation point.

To study this, we used a pre-trained pre-saccadic decoder. Specifically, we used a decoder trained to decode the rewarded-saccade during the pre-saccadic epoch (t: t + Δt where t = −150ms and = −50ms) to decode the saccade direction across the target-fixation and up until the onset of the end-saccade. Importantly, we use the decoder to readout the direction of the end saccade, not of the rewarded saccade and we evaluate the accuracy of the read-outs separately for trials from a single direction of the rewarded saccade. We focus on rewarded saccades to the contralateral hemifield, which are followed by end saccades in many different directions and are thus well-suited to test the decoder (rewarded saccades toward 0, 30 and 60° in Figure 2A, left panel).

Figure 3B shows that post-saccadic activity following the rewarded saccade does not contain preparatory activity for the end saccade, when these behavioral correlations are ''subtracted'' (see histogram of balanced conditions in Figure 3A, right panel), but does contain information about the rewarded saccade. Importantly, the decoding accuracies are computed from the same trials in both cases. Note that it is still possible that preparatory activity of the end saccade would exist along another readout, one that is different from the pre-saccadic readout of the rewarded saccade. Even so, this result shows that the inverted tuning of pre-saccadic activity after saccade execution is not a consequence of the next saccade the monkey will perform.

## Prospective and retrospective representations have different task-selectivity

On some recording days monkeys performed three tasks sequentially: (1) the perceptual decision-making task, where the monkeys had to choose between two targets based on sensory information; (2) the instructed-saccade task, where only one peripheral target was presented on each trial; (3) the non-spatial associative task, where monkeys had to choose between two targets based on information from the previous trial. Targets were placed at identical locations across the three tasks, allowing us to study how task-context modulates responses.

We analyzed responses aligned to target (one target in instructed saccade task, two targets of different colors in the associative task and dots onset in the perceptual task) and saccade onset. We identify choice-decoders that best separate the population responses due to monkey's choices (leftward or rightward) across the three tasks.

Note that because trials within the three tasks are not intermingled, but come in sequential blocks, we corrected the single-trial spike counts of any potential population-level drift in the baseline firing rates:

$$\tilde{x}_{i,t,\mathrm{task}-1} = x_{i,t,task-1} - \langle x_{i,t} \rangle_{task-1}$$

$$\tilde{x}_{i,t,\mathrm{task}-2} = x_{i,t,task-2} - \langle x_{i,t} \rangle_{task-2}$$

$$\tilde{x}_{i,t,\mathrm{task}-3} = x_{i,t,task-3} - \langle x_{i,t} \rangle_{task-3}$$

The decoding analyses was performed on the normalized responses.

### Post-saccadic activity does not encode the momentary gaze location

We addressed the question whether post-saccadic activity is better explained by saccade-covariates or eye-position-covariates in a modified version of the perceptual decision-making task, in which the monkeys were presented with two workspace configurations in a blocked design (Figures 2D and 2E). The task required the monkeys to discriminate the dominant movement of moving dots in two "workspaces" that were retinotopically identical, but horizontally (or vertically) shifted along the monkey's line of sight, such that the physical location of one target (T1) in one block was identical to the physical location of the other target (T2) in the other block.

$$x_{i,t}(k) = \beta_{0,i,t} + \beta_{\text{choice},i,t}\text{choice}(k) + \beta_{\text{gaze},i,t}\text{gaze}(k) + \beta_{\text{gaze}_{\text{abs}},i,t}\text{gaze}_{\text{abs}}(k)$$

where $x_{i,t}(k)$ is the z-scored response of unit i at time t and on trial k, choice(k) is the monkey's choice on trial k (+1 for choice 1 and -1 for choice 2), gaze(k) is the target-location on trial k (for two sessions the workspace is shifted along the horizontal axis gaze = $\text{gaze}_x$ = $\{-1,0,1\}$ and $\text{gaze}_y = 0$; and for two sessions the workspace is shifted along the vertical axis gaze = $\text{gaze}_y = \{-1,0,1\}$ and $\text{gaze}_x = 0$, $\text{gaze}_{\text{abs}}(k)$ is the absolute value of gaze($k$). We introduced $\text{gaze}_{\text{abs}}(k)$ to capture a potential non-linear relation between neural responses and gaze. We focused on three time points in the post-saccadic epoch: early (+50ms), middle (+200ms) and late (+400ms).

Because trials within the two retinotopically-identical sessions, $\text{workspace}_1$ and $\text{workspace}_2$, are not intermingled, but come in sequential blocks, we corrected the single-trial spike counts of any potential population-level drift in the baseline firing rates:

$$\tilde{x}_{i,t,\text{workspace}_1} = x_{i,t,\text{workspace}_1} - \langle x_{i,t}\rangle_{\text{workspace}_1}$$

$$\tilde{x}_{i,t,\text{workspace}_2} = x_{i,t,\text{workspace}_2} - \langle x_{i,t}\rangle_{\text{workspace}_2}$$

We identified the regression coefficients $\beta_{\text{choice},i,t}$, $\beta_{\text{gaze},i,t}$, $\beta_{\text{gaze}_{\text{abs}},i,t}$ through 10-fold cross-validation for each unit separately. We next quantified the saccade-related and gaze-related contributions of each unit through a measure of variance explained on the test trials:

$$\text{variance explained}_{i,t,\text{gaze}} = 1 - \frac{\sum_k \|\tilde{x}_{i,t} - \hat{x}_{i,t,\text{gaze}}\|^2}{\sum_k \left(\tilde{x}_{i,t} - \langle \tilde{x}_{i,t}\rangle_k\right)^2}$$

where

$$\hat{x}_{i,t,\text{gaze}}(k) = \beta_{0,i,t} + \beta_{\text{gaze},i,t}\text{gaze}(k) + \beta_{\text{gaze}_{\text{abs}},i,t}\text{gaze}_{\text{abs}}(k)$$

Similarly for saccade-related activity:

$$\text{variance explained}_{i,t,\text{saccade}} = 1 - \frac{\sum_k \|\tilde{x}_{i,t} - \hat{x}_{i,t,\text{saccade}}\|^2}{\sum_k \left(\tilde{x}_{i,t} - \langle \tilde{x}_{i,t}\rangle_k\right)^2}$$

where

$$\hat{x}_{i,t,\text{saccade}}(k) = \beta_{0,i,t} + \beta_{\text{choice},i,t}\text{choice}(k)$$